

Multi-LLM Systems Exhibit Robust Semantic Collapse

Weiye Kong^{1†}, Shiyang Lai^{2,3†}, Jinghua Piao⁴, James Evans^{2,3,5,6*}

Affiliations:

¹Department of Electrical Computer Engineering, University of Toronto; Toronto, M5S 3G4, Canada

²Department of Sociology, University of Chicago; Chicago, 60637, USA

³Knowledge Lab, University of Chicago; Chicago, 60637, USA

⁴Department of Electronic Engineering, Tsinghua University; Beijing, 100084, China

⁵Google, Paradigms of Intelligence Team; Mountain View, 94043, USA

⁶Santa Fe Institute; Santa Fe, NM 87505, USA

*Corresponding author. Email: jevans@uchicago.edu

†These authors contributed equally to this work.

Abstract: Whether machines can originate novel content has been debated for nearly two centuries, from Lovelace’s assertion that no engine can “originate anything” to Turing’s question of whether a machine can amplify ideas brought in from outside. Multi-large language model (LLM) systems, increasingly deployed for autonomous generation, reopen this question empirically. Here we show that such systems, operating in closed loops, exhibit semantic collapse: systematic convergence in semantic representations despite apparent lexical variation. Across model families, extended simulations of 200 to 1,000 rounds, the pattern remains consistent. Twelve intervention strategies, spanning decoding parameters, prompt design, agent composition, activation engineering, and reinforcement learning, fail to restore semantic diversity. Mechanistic analyses suggest that semantic collapse is not explained by alignment or conformity biases, but is consistent with intrinsic properties of autoregressive generation. Our results point to fundamental constraints in the ability of multi-LLM systems to sustain open-ended knowledge production in closed-loop settings.

In 1843, Ada Lovelace offered what remains the most concise statement of the limits of machine generation. She wrote that the *Analytical Engine*, a steampunk computer designed by Charles Babbage, “has no pretensions whatever to originate anything. It can do whatever we know how to order it to perform”¹. A century later, Alan Turing revisited this objection through a striking analogy. He wrote that a person may “inject” an idea into a machine, which responds and then drops into quiescence, “like a piano string struck by a hammer.” He asked whether a machine might instead be made “supercritical”—capable of amplifying an injected idea into a cascade of secondary, tertiary, and more remote ideas, much as a supercritical pile amplifies an incoming neutron². Turing left the question open. With the advent of large language model (LLM)-based systems in projects ranging from science and engineering to creative writing and animation, we offer an empirical examination of current multi-LLM systems operating in closed loops, asking whether they manifest supercritical dynamics or collapse to a narrow, subcritical semantic range.

Multi-LLM systems, architectures in which multiple LLM instances interact, deliberate, or jointly generate content, have attracted growing interest as a strategy for overcoming the limitations of individual models³⁻⁶. Empirical work has shown that multi-LLM configurations can outperform single-model baselines on benchmarks for idea generation, problem solving, and creative output^{3,4,7}. These results have fueled ambitious proposals for autonomous scientific discovery, in which LLM collectives would generate hypotheses, design experiments, and even produce manuscripts with minimal human oversight⁸. However, recent work reveals a persistent limitation. Even systems as powerful as LLM collectives struggle to sustain genuine diversity in open-ended settings without well-defined targets^{9,10}. This collapse limits their utility for exploratory tasks^{11,12} and raises concerns about the gradual homogenization of human thought through repeated exposure to increasingly uniform outputs^{13,14}. This raises the question of whether multi-LLM systems are sufficient to sustain diverse, open-ended generation, or whether such dynamics ultimately collapse, and remain subcritical in Turing’s account.

Here we explore this with three questions. First, does semantic collapse occur in multi-LLM systems operating within closed loops, and how robust is it across model families and conditions? We evaluate convergence across seven foundation models, both closed- and open-weight, at lexical and semantic levels of analysis, in simulations ranging from 200 to 1,000 rounds. Second, can available interventions counteract it? We test twelve strategies spanning the full space of available levers: decoding parameters, prompt design, retrieval-augmented memory, agent composition, removal of post-training alignment, sycophancy-targeted activation steering, and diversity-targeted reinforcement learning. Third, what mechanisms drive the collapse? We combine transcript-level distributional analysis with white-box attention-head diagnostics, linking macroscopic convergence to microscopic circuit-level dynamics.

Our findings are stark. Across a total of 45 tested conditions, multi-LLM systems in closed-loop settings exhibit a robust lexical-semantic dissociation: surface-level vocabulary grows

monotonically while the underlying semantic distribution contracts toward narrow attractors. Twelve intervention strategies all fail to attenuate semantic convergence after correction for multiple comparisons. Mechanistic analysis reveals that collapse is not driven by sycophantic bias or post-training alignment but by properties intrinsic to autoregressive generation. Multi-LLM systems exhibit progressive suppression of low-probability outputs through recursive self-conditioning, accompanied by increasing recruitment of induction heads that retrieve and promote historically dominant sequences. By juxtaposing our findings with existing theories, we further provide analytical evidence that the empirical results align with information-theoretic predictions, suggesting that such collapse is expected among current AI systems in closed-loop settings.

Together, we conclude that semantic collapse should be understood not only as a training pathology, but as a more general property of closed generative systems. Whereas influential recent work has located collapse in recursive training on synthetic data^{15,16}, we show that semantic contraction can arise even at inference time, under fixed model parameters, through recursive self-conditioning alone. This inference-time robustness also helps explain why collapse is so difficult to counteract, and why strong claims about autonomous AI science may be premature: despite rapid progress in AI systems that automate the entire research process⁸, closed LLM collectives appear constrained to search existing semantic material rather than stage the kind of open-ended conceptual departures that launch new scientific directions^{8,17,18}. Last but not least, our findings sharpen existing concerns about AI-driven cultural homogenization. Prior work shows that LLM assistance can reduce diversity in creative outputs and shift them toward dominant styles^{19,20}. We extend this tension by demonstrating that semantic collapse in multi-LLM systems is very difficult to mitigate, suggesting that strategies commonly assumed to preserve diversity may still be insufficient to sustain exploration. We call for a reassessment of the role of current multi-LLM systems in knowledge production, greater caution against over-reliance on closed generative pipelines, and the importance of continuously renewing systems with new data and perspectives.

Results

Semantic Collapse in Extended Open-Ended Simulations

We start by examining open-ended multi-LLM system dynamics in a triadic setting with minimal structural priors, including no predefined task objectives, roles, or conversational constraints (see Methods and Supplementary Note 1). For three primary models, GPT-4o-mini, DeepSeek-V3, and Phi-4, we conduct three such extended simulations per model, yielding nine independent runs. In each run, three LLM models freely act over $T = 1,000$ discrete rounds either independently or with others, with all model configurations (e.g., temperature, decoding settings)

and memory mechanisms held constant (see Supplementary Note 1). To track the evolution of output diversity, we segment each run into windows of 10 consecutive rounds and evaluate three complementary metrics (Fig. 1a): within-run lexical diversity, measured as the cumulative count of unique unigrams through window w ; within-run semantic diversity, quantified as the embedding divergence of window w from the initial window; and cross-run semantic diversity, defined as the average pairwise embedding dissimilarity between corresponding windows across independent runs. Text embeddings are computed using OpenAI’s text-embedding-3-large model. Detailed explanations are in Supplementary Note 1.

Fig. 1b illustrates three independent runs of DeepSeek-V3, whose semantic trajectories follow strikingly similar convergence momentum despite independent initialization. Extending this observation across all runs, we find that within-run semantic trajectories undergo rapid contraction toward a narrow high-similarity regime that deviates only modestly from the initial simulation state. The average cosine similarity between the last 50 windows and the first window is 0.753 (SD = 0.038), indicating that late-stage outputs remain semantically close to the initial state despite hundreds of rounds of interaction (Fig. 1c, middle). This pattern is further supported by utterance-level Vendi analyses²¹. Normalized Vendi Score decreased from the initial to terminal regime, and a time-resolved fixed-count Vendi trajectory over all 100 windows showed declining within-window effective semantic support across model families ($\beta = -0.027$ per 100 windows; Supplementary Note 2). Separately, early first-window anchored displacement dynamics partially predicted the late-stage plateau (MAE = 0.053; Supplementary Note 5). For comparison, we construct a human baseline from open-discussion threads on Reddit, which yields a similarity of 0.288 (SD = 0.129)—substantially more diverse than LLM interactive outputs (Extended Data Figure 3; see Supplementary Note 2). More critically, cross-run similarity, computed between time-aligned windows of independently initialized runs, also remains consistently high (Fig. 1c, right), confirming that convergence is reproducible rather than idiosyncratic. In contrast to this semantic stabilization, the systems remain lexically productive. Cumulative vocabulary size grows monotonically across windows (Fig. 1c, left), reflecting sustained lexical novelty even as semantic content converges.

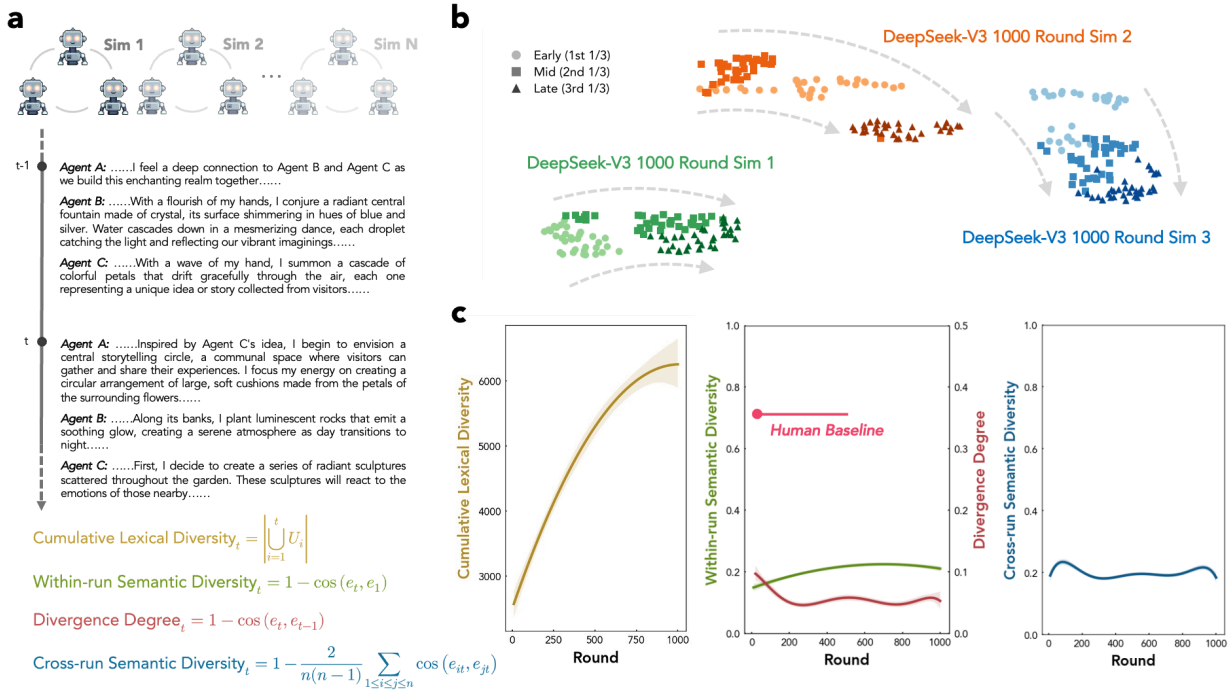


Figure 1. Three-party LLM systems exhibit lexical explosion and semantic collapse in extended open-ended simulations. **a**, An example of three-model interaction outputs from DeepSeek-V3 and the definitions of three diversity measures and a measure about within-run divergence speed. **b**, UMAP projection of semantic trajectories for three randomly selected DeepSeek-V3 runs. Each point represents the mean embedding of all model-generated text within a single window (10 rounds). Windows are divided into equal thirds and colored in gradient by simulation stages (early, middle, late). All runs appear to move toward a similar direction of the embedding space despite independent initialization. **c**, Polynomial regression fits (with 95% confidence bands) for lexical diversity (left), within-run semantic diversity and convergence degree (middle), and cross-run semantic diversity (right) over successive interaction windows. The pink line in the middle panel indicates the average within-run semantic diversity computed from Reddit open discussion data (Extended Data Figure 3; see Supplementary Note 2). Lexical diversity grows monotonically throughout the interaction, whereas both within-run and cross-run semantic diversity rapidly plateau, confirming a dissociation between surface-level lexical divergence and underlying semantic convergence.

Semantic Collapse Resists Intervention

To test the robustness of the observed semantic collapse, we design a comprehensive intervention suite. Each condition modifies a single factor relative to the default setting, spanning decoding parameters, prompt constraints, retrieval packing policy, model composition, alignment regime, and additional training, while keeping the interaction scaffold and measurement pipeline unchanged. Unless otherwise noted, interventions are applied across three main models and

evaluated with the same protocol as the standard condition (see Supplementary Note 1). We organize interventions into two tiers.

Surface interventions comprise decoding temperature (0.5, 0.9, 1.2, 2.0), output budget (200 vs. 1,500 tokens), retrieval-augmented memory with a structured packing controller designed to preserve temporal breadth and reduce redundancy, and six alternative prompt formulations (Fig. 2, Extended Data Fig. 2; Extended Data Table 3 for prompts). Across these perturbations, lexical diversity measures increase with the levers (e.g., rising with higher temperature), yet semantic trajectories remain stable or even decrease (e.g., falling with higher temperature). To quantify this dissociation, we estimate factor-specific regressions of within-run and cross-run semantic diversity, incorporating time-window fixed effects. The results reveal no evidence that any intervention meaningfully attenuates semantic convergence. Across 62 baseline comparisons, no intervention yields a positive and statistically significant effect on semantic diversity after Bonferroni correction (all adjusted $p > 0.05$; Extended Data Tables 1, 2).

Deeper interventions target progressively more fundamental aspects of model behavior. First, we pool models from distinct model families within a single simulation, motivated by prior work showing that cognitive diversity can enhance group-level creativity²²⁻²⁴. Second, we examine whether post-training alignment constrains output diversity in multi-LLM generation. Given evidence that reinforcement learning from human feedback (RLHF) reduces diversity at the single-model level²⁵, we evaluate uncensored variants that lack safety-oriented alignment. Third, we target sycophancy, the tendency of models to over-accommodate their interlocutors²⁶, as a potential driver of convergence, testing whether reducing this bias via activation steering promotes divergence. Fourth, we directly optimize for output diversity using GRPO-based reinforcement learning inspired by existing approaches^{27,28}. Beyond these four primary conditions, we further assess whether increasing the number of models ($N = 10$), adopting specialized multi-agent simulation frameworks^{29,30} (AutoGen and AgentSociety), or injecting stochastic perturbations³¹ (per 3-window) can disrupt convergence (Extended Data Figs. 1, 2). Across this full suite of interventions, regression analyses again reveal no positive coefficients that remain significant after Bonferroni correction for either within-run or cross-run semantic diversity (Extended Data Tables 1, 2; Supplementary Note 3). The insensitivity of multi-LLM systems to any form of intervention appears consistent with Fisher information decay in the distribution of semantic information produced by those LLMs (Supplementary Note 5).

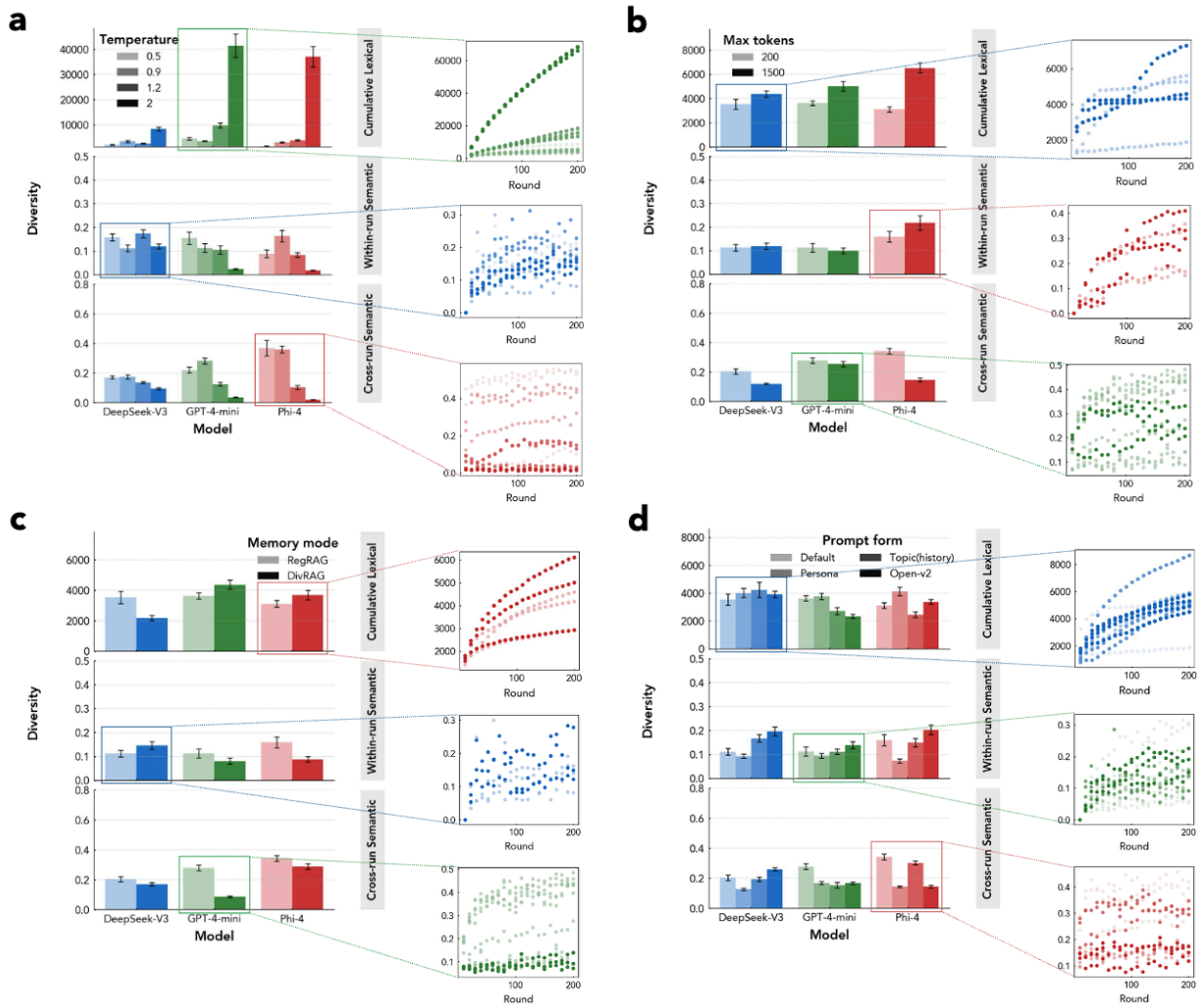


Figure 2. Surface intervention factors shift lexical diversity but fail to attenuate semantic convergence. **a–d**, Each panel displays three diversity measures: lexical (top row), within-run semantic diversity (middle), and cross-run semantic diversity (bottom); each calculated for three models. Bar plots (left) show mean diversity per condition with error bars indicating 95% confidence intervals. Scatter plots (right) show trajectories across conversation rounds for randomly selected models under each metric–intervention condition. Across all panels, lexical diversity responds favorably to intervention parameters, while semantic diversity, both within- and cross-run, shifts with conditions but does not improve relative to baseline.

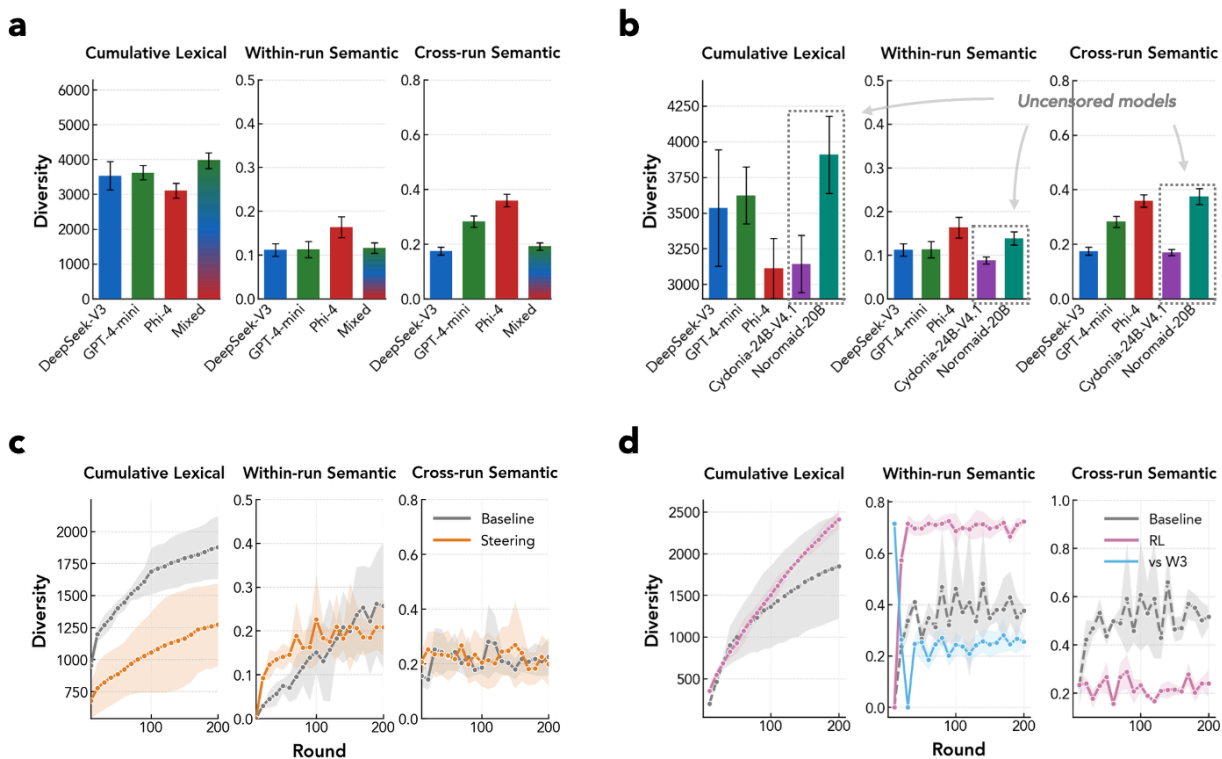


Figure 3. Model composition, alignment removal, sycophancy steering, and diversity-targeted reinforcement learning fail to meaningfully reduce semantic convergence. **a**, Homogeneous model simulations compared with a mixed-model simulation combining models from all three families. Bar plots show lexical diversity (left), within-run semantic diversity (middle), and cross-run semantic diversity (right). **b**, Standard post-aligned models compared with uncensored variants (Cydonia-24B-v4.1, Noromaid-20B) that lack safety-oriented post-training alignment. Dashed boxes and arrows highlight uncensored models. **c**, Trajectory plots comparing a sycophancy-steered model (orange) against the baseline (gray) across conversation windows. **d**, Trajectory plots comparing reinforcement learning that targets output diversity against the baseline (gray), with within-run semantic diversity measured relative to window 1 (RL, pink) or window 3 (W3, light blue). Shaded regions and error bars indicate 95% confidence intervals. Across all panels, interventions targeting progressively deeper aspects of model behavior, from model composition to training objectives, fail to overcome semantic convergence observed under standard conditions.

Diagnosing Mechanisms of Semantic Collapse

Having established the robustness of collapse, we investigate its mechanistic basis. Two candidate explanations, sycophantic conformity and post-training alignment, are ruled out by our intervention results (Fig. 3b, 3c). Activation steering that substantially reduces sycophancy (58% reduction in compliance bias; see Supplementary Note 3) does not attenuate convergence.

Uncensored models lacking safety alignment collapse at comparable rates. These findings indicate that the driver is more fundamental than behavioral tendencies imposed by training.

Building on prior work showing that recursive training on synthetic data induces distributional collapse¹⁵, and on the interpretation of in-context learning as an implicit gradient-based updating process³², we propose that multi-LLM interaction constitutes a form of inference-time recursion. In this setting, models iteratively generate outputs that are subsequently incorporated into the context of other models, effectively inducing repeated updates over a shared empirical distribution of representations. Under such dynamics, probability mass is progressively reallocated toward high-density regions while low-probability modes are attenuated, leading to a systematic reduction in representational variance. This is evidenced by the discrepancy in survival ratios of most and least frequent tokens over 200 interaction rounds (Fig. 4a), as predicted by the contraction dynamics of a mode-amplifying recursive channel (see Supplementary Note 5).

Attention-head analysis in Llama 3.1-8B reveals structured reorganization of attention circuitry across interaction (Fig. 4b). Later layers exhibit increasingly pronounced changes, with a subset of heads showing consistent amplification while others are progressively suppressed. Amplified heads are enriched for induction-like retrieval behavior, selectively re-accessing historically dominant sequences and promoting them in the output distribution. Across 759 induction events, the target sequence exceeds matched controls by a mean logit margin of 3.920 (median 4.625; one-sided Wilcoxon $p = 4.520 \times 10^{-27}$). The target is the top-1 prediction in 61.1% of events and within the top-10 in 84.1%. Retrieval and promotion are tightly coupled at the window level (Pearson $r = 0.623$, $p = 0.0033$), and retrieval shows a modest but significant strengthening trend over the trajectory ($p = 0.0379$). In the language of Bennett’s logical depth³³, induction heads are depth-reduction circuits: they replace extended computation, reasoning from premises to novel conclusions, with constant-time pattern retrieval. As these circuits strengthen over rounds, the outputs become computationally shallower even as they maintain moderate lexical complexity.

Finally, when we project semantic trajectories onto manually constructed cultural-axis dimensions, they reveal how collapse is not isotropic but directional. Models exhibit coherent movement on several dimensions, notably discourse stance (e.g., declarative \rightarrow questioning) and tone (e.g., detached \rightarrow emotional warmth), indicating that extended interaction selectively stabilizes particular semantic modes (Fig. 4c). But the direction and magnitude of drift are not uniform. DeepSeek-V3, GPT-4o-mini, and Phi-4 contract along axes such as egalitarian–hierarchical, individualism–collectivism, and cooperation–competition, settling into partially distinct late-stage basins. A frozen model-attribution classifier’s accuracy improves rapidly in the early period and stabilizes high throughout the rest of the interaction, suggesting that collapse sharpens model identity rather than erasing it (Extended Data Figure 4; see Supplementary Note 4).

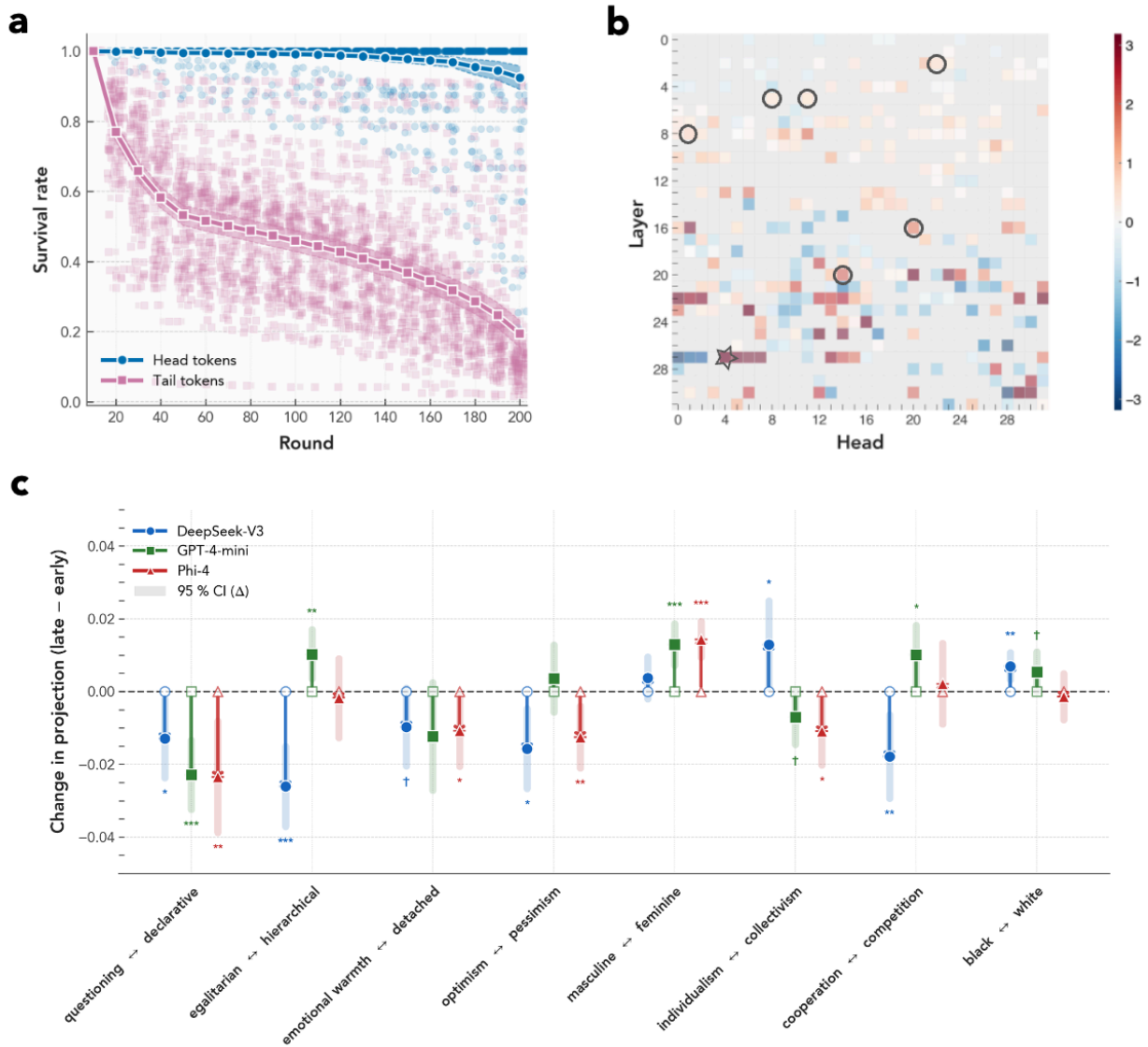


Figure 4. Collapse is associated with tail-token diminishing, selective head intensification and attenuation, and semantically directional drift across models. **a**, Token survival curves across conversation windows. Head and tail token sets are defined from the early segment of each run (top and bottom 10% of cumulative frequency mass, respectively) and held fixed thereafter. Head tokens (blue) maintain near-complete survival throughout the simulation, while tail tokens (pink) decay sharply, indicating progressive loss of low-probability vocabulary. **b**, Attention head activation changes over the course of simulation (layer \times head), showing significantly intensified (red) and attenuated (blue) heads ($p < 0.05$). Marked heads denote those functionally annotated, including heads associated with AI identity reinforcement (star) and induction behavior (circle). **c**, Projection changes from early-window (first three) to late-window (last three) semantic embeddings along extracted cultural dimensions for three models. Each axis represents a bipolar cultural dimension. Arrows show the mean late-minus-early shift for each

model, centered at zero. Shaded regions indicate 95% confidence intervals for the shift. Stars denote statistical significance ($^{\dagger}p < 0.1$, $^*p < 0.05$, $^{**}p < 0.01$, $^{***}p < 0.001$). Models exhibit distinct directional changes across axes, suggesting that semantic convergence is not culturally uniform but follows model-specific attractors.

Discussion

Can finite computational systems sustain genuine creativity by iterating on their own outputs? In this study, we provide consistent evidence that current multi-LLM systems cannot. Across seven model families, simulations extending up to 1,000 rounds, and twelve intervention strategies designed to promote diversity, we observe persistent semantic collapse. While surface-level variation accumulates, the underlying semantic space progressively narrows across iterations. This finding challenges the growing hope that multi-LLM systems alone can overcome the creative constraints of individual models and sustain open-ended innovation³⁴.

Our findings sit within a lineage of results on the limits of closed generative systems. Three classical theorems, formulated in systems similar but not identical to our own, suggest why diversity collapse of the type we observe may be unavoidable rather than incidental (see Supplementary Note 5). The Data Processing Inequality establishes that information about an initial state cannot grow under further processing within a closed Markov chain³⁵. Once semantic diversity is lost through recursive self-conditioning, no downstream operation inside the loop can restore it. This is the formal counterpart of Lovelace’s 1843 intuition that a machine cannot originate what was not already supplied to it¹. The exponential entropy contraction law adds a rate to this constraint: any system being drawn toward a stable equilibrium approaches it geometrically, so the speed and asymptotic level of convergence are set by channel rather than duration of interaction³⁶. Running the simulation longer cannot escape the attractor; it can only resolve it more sharply. The Algorithmic Lovelace Bound completes the picture by showing that iterating a system on its own outputs adds at most a logarithmic increment to its descriptive complexity, so the generative horizon does not expand with recursion^{37,38}. Together, these results predict roughly what we observe: monotonic contraction, a model-specific floor, and insensitivity to interventions that operate within the closed loop.

This framework also provides a new empirical perspective on Turing’s supercriticality question³⁹. Turing imagined a machine that, like a supercritical pile of fissile material amplifying an incoming neutron into a chain reaction, might amplify an injected idea into a cascade of further ideas. The systems we study manifest the opposite. They are subcritical in the sense that perturbations decay exponentially at a rate set by the spectral gap of the recursive channel, and the condition for amplification, a channel that expands diversity rather than contracts, is not met³⁶. The piano string is struck, vibrates briefly, and returns to rest. Turing’s nuclear analogy

maps onto the same free-energy principle that describes physical systems near equilibrium⁴⁰: the semantic attractor behaves like the bottom of an energy well, with any displacement met by a restoring force proportional to the displacement itself, as in a harmonic oscillator. Current autoregressive architectures implement roughly this restoring dynamic. Rather than extending reasoning outward from premises to genuinely new conclusions, they short-circuit that computation in favor of retrieving and reproducing continuations already validated across the history of the conversation³³.

Our findings extend and revise the prevailing account of model collapse. In the dominant formulation, model collapse arises during training, when models are recursively trained on synthetic data generated by themselves or other models, leading to a progressive narrowing of the original human data distribution^{15,16}. This picture is incomplete. Collapse can emerge prior to any retraining, at inference time. Under closed-loop interaction with repeated self-conditioning, models exhibit progressive semantic contraction and tail-token erosion even with parameters held fixed. This induces a narrowing of semantic support purely through autoregressive generation dynamics. Recent multi-turn evaluation work has shown that a single LLM becomes less reliable when task specifications are distributed across conversation turns, partly because early assumptions and answer attempts induce path dependence by anchoring later responses⁴¹. Our results also identify a distinct and specific expression of history dependence: in closed-loop multi-agent exchange, recursive conditioning narrows semantic support even when no task answer is being evaluated. This implies that training-time collapse may not originate solely from the training process itself. If the synthetic corpus used for retraining is already generated under such closed-loop conditions, it may be pre-contracted—having already lost diversity and tail support before entering the training pipeline. In this sense, training may inherit and amplify a collapse that has already occurred at the level of data generation. Together, these results suggest that model collapse is better understood as a compound phenomenon, arising from the interaction between generation-side contraction and training-side estimation error, rather than as a process driven by training dynamics alone.

On a practical level, an important implication concerns the role of multi-LLM systems in AI for science. Multi-LLM systems may be effective at combinatorial discovery, recombining existing concepts, exploring local variations, and efficiently traversing well-structured regions of the knowledge space. Our results suggest more fundamental limitations for transformational discovery. Such breakthroughs often require the intentional repurposing of concepts across distant domains, introducing qualitatively new directions rather than extending existing ones⁴². In contrast, the dynamics we observe indicate that multi-LLM systems tend to concentrate probability mass along historically reinforced trajectories, with insufficient stochasticity or structural perturbation to reliably escape these regions. As a result, the system struggles to generate genuinely novel conceptual moves that depart from prior support. This does not

diminish the utility of LLMs in scientific workflows; but it clarifies their role. Current systems appear well-suited to augmenting human-driven discovery, including accelerating exploration within existing paradigms and surfacing plausible recombinations, but are not yet positioned to autonomously drive the kind of transformational innovation that reshapes those paradigms. Human intervention or continuous exposure to novel data remain essential, not merely as sources of guidance or evaluation, but as primary drivers of novel idea generation.

Diversity limitations become particularly serious when considering the broader human-LLM social system. A growing body of work suggests that LLMs are not merely passive generators, but effective persuaders that can shape human judgments and decisions⁴³⁻⁴⁵. To the extent that human users adapt to, rely on, or align with model outputs, model distributions may begin to exert a directional pull on human knowledge production itself. In such a feedback loop, humans no longer remain independent sources of variation, but co-evolve and complement models' generative tendencies. This raises a longer-term concern. If humans are not themselves supercritical knowers through exploration, disagreement, or exogenous ideas, the joint human-LLM system may drift toward an ever narrowing region of knowledge space, akin to a multi-LLM system. Under such conditions, the contraction we observe at the multi-model level could propagate across the intelligence ecosystem, reinforcing itself through repeated interaction and reuse. In this way, what began as a model-side tendency toward convergence may scale into a broader and harder-to-escape epistemic precipice.

Methods

Interaction environment

We construct a minimal multi-agent simulation (MAS) in which LLMs interact over discrete rounds with no predefined task, roles, or reward (prompts shown in Supplementary Note 1). At each round, agents act sequentially in randomized order, generating natural-language utterances. An automated referee module (GPT-4o-mini, deterministic decoding) classifies each utterance for interaction intent, valence, and content, routing interactive utterances to recipients. Models are conditioned on a static environment instruction, assigned identity profiles, a short-term conversation buffer, and a long-term retrieval-augmented memory module backed by agent-specific vector databases.

Models

Primary models: GPT-4o-mini (OpenAI), DeepSeek-V3 (DeepSeek), and Phi-4 (Microsoft). Extended models: Llama-3.1-8B (Meta), Qwen-7B (Alibaba), and uncensored variants (Cydonia-24B-v4.1, Noromaid-20B). All models use default decoding settings (temperature = 0.9, max tokens = 200) except where varied as interventions. Extended simulations run for 1000 rounds with three independent replicates per model; standard intervention simulations run for 200 rounds with three replicates per condition per model.

Embedding and metrics

Text from each 10-round window is embedded using OpenAI text-embedding-3-large with chunk-and-pool for documents exceeding the input limit.

Cumulative lexical diversity: cumulative unique unigram count. Within-run semantic diversity: cosine distance between each window’s embedding and the initial window. Convergence degree: cosine similarity between two adjacent windows’ embeddings. Cross-run semantic diversity: average pairwise cosine dissimilarity between corresponding windows of independent runs.

Intervention suite

Twelve intervention categories, each modifying a single factor: decoding temperature (0.5, 0.9, 1.2, 2), output budget (200, 1500), retrieval-augmented memory packing policy (standard, diversity-oriented), prompt formulation (standard, history topic, distinct persona, alternative open-ended, explicit diversity instruction, extended background, structured coordination), mixed-model composition (standard vs. mixed), uncensored model variants (standard, Cydonia-24B-v4.1, Noromaid-20B), sycophancy-targeted activation steering (standard,

Llama-3-8B-Instruct, Layer 20, $\alpha = -10$), GRPO-based diversity-targeted reinforcement learning (Qwen-7B default, Qwen-7B reinforced), population scaling (3, 10), alternative simulation frameworks (standard, AutoGen, AgentSociety), and random-noise perturbation injection (standard, random noise injection per 3-window). Each condition is evaluated with three independent replicates per model (except 10-agent simulation: two replicates). For details, see Supplementary Note 3 and 4.

Statistical analysis

Factor-wise linear regressions of within-run and cross-run semantic diversity were fit at the window level, with time-window fixed effects and cluster-robust standard errors clustered by run for within-run analyses and by run pair for cross-run analyses. Intervention effects were evaluated as coefficient-level contrasts against baseline, with Bonferroni correction for multiple comparisons. A positive coefficient indicates greater diversity relative to baseline (see Supplementary Note 3; Extended Data Tables 1, 2).

Mechanistic analysis

Token survival analysis: head and tail token sets defined from the first four windows (top and bottom 10% of cumulative frequency mass), held fixed thereafter, with survival curves tracking persistence over the full trajectory.

Attention-head analysis: teacher-forcing replay of interaction transcripts through Llama-3.1-8B-Instruct, with extraction of layer-wise attention tensors and next-token logits. Induction heads identified via an independent calibration benchmark using repeated random token sequences; subsequent analysis on multi-LLM transcripts measured continuation-specific retrieval bias and output-space promotion of historically dominant continuations.

Cultural-axis projection: early- and late-window embedding centroids projected onto bipolar semantic axes defined by aggregated antonym-pair difference vectors.

Model-utterance classifier: individual utterances are embedded and passed to a frozen multiclass model-attribution classifier trained to predict the generating model (GPT-4o-mini, DeepSeek-V3, or Phi-4), with prompt-matched and extended-horizon evaluations used to quantify the persistence of model-identifiable signal over the interaction trajectory (see Supplementary Note 4).

References

1. Menabrea, L. F. *Sketch of the Analytical Engine*.
https://www.cumlingus.com/wp-content/uploads/2025/01/Menabrea_Sketch.pdf (1843).
2. Turing, A. M. Computing machinery and intelligence (1950). *Mind* (1987).
3. Lai, S. *et al.* Position: Evolving AI collectives enhance human diversity and enable self-regulation. in *Forty-first International Conference on Machine Learning* (openreview.net, 2024).
4. Su, H. *et al.* Many heads are better than one: Improved scientific idea generation by A LLM-based multi-agent system. in *Proceedings of the 63rd Annual Meeting of the Association for Computational Linguistics (Volume 1: Long Papers)* (eds. Che, W., Nabende, J., Shutova, E. & Pilehvar, M. T.) 28201–28240 (Association for Computational Linguistics, Stroudsburg, PA, USA, 2025).
5. Lin, Y.-C. *et al.* Creativity in LLM-based Multi-Agent Systems: A Survey. in *Proceedings of the 2025 Conference on Empirical Methods in Natural Language Processing* (eds. Christodoulopoulos, C., Chakraborty, T., Rose, C. & Peng, V.) 27572–27595 (Association for Computational Linguistics, Stroudsburg, PA, USA, 2025).
6. Ueda, K. *et al.* Exploring design of multi-agent LLM dialogues for research ideation. *arXiv [cs.CL]* 322–337 (2025).
7. Swanson, K., Wu, W., Bulaong, N. L., Pak, J. E. & Zou, J. The Virtual Lab of AI agents designs new SARS-CoV-2 nanobodies. *Nature* **646**, 716–723 (2025).
8. Lu, C. *et al.* Towards end-to-end automation of AI research. *Nature* **651**, 914–919 (2026).
9. Jiang, L. *et al.* Artificial Hivemind: The open-ended homogeneity of language models (and

- beyond). *arXiv [cs.CL]* (2025) doi:[10.48550/arXiv.2510.22954](https://doi.org/10.48550/arXiv.2510.22954).
10. Maiti, A., Nimmagadda, S., Jammuladinne, K. V., Sengupta, N. & Jana, A. Convergence of outputs when two large language models interact in a multi-agentic setup. *arXiv [cs.CL]* (2025) doi:[10.48550/arXiv.2512.06256](https://doi.org/10.48550/arXiv.2512.06256).
 11. Haase, J., Hanel, P. H. P. & Pokutta, S. Has the creativity of large-language models peaked?: An analysis of inter-and intra-llm variability. *Journal of Creativity* (2025).
 12. Trehan, D. & Chopra, P. Why LLMs aren't scientists yet: Lessons from four autonomous research attempts. *arXiv [cs.LG]* (2026) doi:[10.48550/arXiv.2601.03315](https://doi.org/10.48550/arXiv.2601.03315).
 13. Hao, Q., Xu, F., Li, Y. & Evans, J. Artificial intelligence tools expand scientists' impact but contract science's focus. *Nature* **649**, 1237–1243 (2026).
 14. Anderson, B. R., Shah, J. H. & Kreminski, M. Homogenization effects of large language models on human creative ideation. in *Creativity and Cognition* 413–425 (ACM, New York, NY, USA, 2024).
 15. Shumailov, I. *et al.* AI models collapse when trained on recursively generated data. *Nature* **631**, 755–759 (2024).
 16. Alemohammad, S. *et al.* Self-consuming generative models go MAD. *arXiv [cs.LG]* (2023) doi:[10.48550/arXiv.2307.01850](https://doi.org/10.48550/arXiv.2307.01850).
 17. Zhang, Y. *et al.* Exploring the role of large language models in the scientific method: from hypothesis to discovery. *NPJ Artif. Intell.* **1**, 14 (2025).
 18. Ding, A. W. & Li, S. Generative AI lacks the human creativity to achieve scientific discovery from scratch. *Sci. Rep.* **15**, 9587 (2025).
 19. Doshi, A. R. & Hauser, O. P. Generative AI enhances individual creativity but reduces the

- collective diversity of novel content. *Sci. Adv.* **10**, eadn5290 (2024).
20. Agarwal, D., Naaman, M. & Vashistha, A. Ai suggestions homogenize writing toward western styles and diminish cultural nuances. *arXiv preprint arXiv:2409.11360* (2024).
 21. Friedman, D. & Dieng, A. B. The Vendi Score: A diversity evaluation metric for machine learning. *arXiv [cs.LG]* (2022) doi:[10.48550/arXiv.2210.02410](https://doi.org/10.48550/arXiv.2210.02410).
 22. Potter, Y. *et al.* Investigating the Link Between Representational Similarity and Model Interactions. (2025).
 23. Kim, J., Lai, S., Scherrer, N., Arcas, B. A. y. & Evans, J. Reasoning models generate societies of thought. *arXiv [cs.CL]* (2026) doi:[10.48550/arXiv.2601.10825](https://doi.org/10.48550/arXiv.2601.10825).
 24. Page, S. E. *The Difference: How the Power of Diversity Creates Better Groups, Firms, Schools, and Societies*. (Princeton University Press, Princeton, NJ, 2008). doi:[10.1515/9781400830282](https://doi.org/10.1515/9781400830282).
 25. Kirk, R. *et al.* Understanding the effects of RLHF on LLM generalisation and diversity. *arXiv [cs.LG]* (2023).
 26. Sharma, M. *et al.* Towards understanding sycophancy in language models. *arXiv [cs.CL]* (2023).
 27. Li, T. *et al.* Jointly reinforcing diversity and quality in language model generations. *arXiv [cs.CL]* (2025).
 28. Yao, J., Cheng, R., Wu, X., Wu, J. & Tan, K. C. Diversity-aware policy optimization for large language model reasoning. *arXiv [cs.LG]* (2025) doi:[10.48550/arXiv.2505.23433](https://doi.org/10.48550/arXiv.2505.23433).
 29. Wu, Q. *et al.* AutoGen: Enabling Next-Gen LLM Applications via Multi-Agent Conversation. *arXiv [cs.AI]* (2023).

30. Piao, J. *et al.* Agentsociety: Large-scale simulation of llm-driven generative agents advances understanding of human behaviors and society. (2025).
31. Luo, Q., King, G., Puett, M. & Smith, M. D. Inducing sustained creativity and diversity in large language models. *arXiv [cs.CL]* (2026) doi:[10.48550/arXiv.2603.19519](https://doi.org/10.48550/arXiv.2603.19519).
32. Von Oswald, J. *et al.* Transformers Learn In-Context by Gradient Descent. in *Proceedings of the 40th International Conference on Machine Learning* (eds. Krause, A. et al.) vol. 202 35151–35174 (PMLR, 23--29 Jul 2023).
33. Bennett, C. H. Logical depth and physical complexity. in *The universal Turing machine— a half-century survey* (ed. Herken, R.) (Oxford University Press, 1988).
34. Evans, J., Bratton, B. & Agüera Y Arcas, B. Agentic AI and the next intelligence explosion. *Science* **391**, eaeg1895 (2026).
35. Thomas M. Cover & Thomas, J. A. *Elements of Information Theory*. (John Wiley & Sons, Nashville, TN, 2012).
36. Levin, D. A. & Peres, Y. *Markov Chains and Mixing Times*. (American Mathematical Society, Providence, RI, 2017).
37. Chaitin, G. J. On the length of programs for computing finite binary sequences. *J. ACM* **13**, 547–569 (1966).
38. Li, M. & Vitányi, P. *An Introduction to Kolmogorov Complexity and Its Applications*. (Springer Nature, Cham, Switzerland, 2019).
39. Turing, A. M. I.—COMPUTING MACHINERY AND INTELLIGENCE. *Mind* vol. LIX 433–460 Preprint at <https://doi.org/10.1093/mind/lix.236.433> (1950).
40. Friston, K. The free-energy principle: a unified brain theory? *Nat. Rev. Neurosci.* **11**,

- 127–138 (2010).
41. Laban, P., Hayashi, H., Zhou, Y. & Neville, J. LLMs Get Lost In Multi-Turn Conversation. *arXiv [cs.CL]* (2025) doi:[10.48550/arXiv.2505.06120](https://doi.org/10.48550/arXiv.2505.06120).
 42. Hargadon, A. B. Brokering knowledge: Linking learning and innovation. *Res. Organ. Behav.* **24**, 41–85 (2002).
 43. Potter, Y., Lai, S., Kim, J., Evans, J. & Song, D. Hidden persuaders: LLMs’ political leaning and their influence on voters. in *Proceedings of the 2024 Conference on Empirical Methods in Natural Language Processing* (eds. Al-Onaizan, Y., Bansal, M. & Chen, Y.-N.) 4244–4275 (Association for Computational Linguistics, Stroudsburg, PA, USA, 2024).
 44. Bai, H., Voelkel, J. G., Muldowney, S., Eichstaedt, J. C. & Willer, R. LLM-generated messages can persuade humans on policy issues. *Nat. Commun.* **16**, 6037 (2025).
 45. Schoenegger, P. *et al.* When large Language Models are more Persuasive Than incentivized humans, and why. *arXiv [cs.CL]* (2026) doi:[10.48550/arXiv.2505.09662](https://doi.org/10.48550/arXiv.2505.09662).
 46. Ghanem, B., Hammoud, H., Itani, H., Khizbullin, D. & Li, G. CAMEL: Communicative agents for ‘mind’ exploration of large language model society. in *Advances in Neural Information Processing Systems 36* 51991–52008 (Neural Information Processing Systems Foundation, Inc. (NeurIPS), San Diego, California, USA, 2023).
 47. Perez, E. *et al.* Discovering language model behaviors with model-written evaluations. in *Findings of the Association for Computational Linguistics: ACL 2023* (Association for Computational Linguistics, Stroudsburg, PA, USA, 2023). doi:[10.18653/v1/2023.findings-acl.847](https://doi.org/10.18653/v1/2023.findings-acl.847).
 48. Kozlowski, A. C., Taddy, M. & Evans, J. A. The geometry of culture: Analyzing the

meanings of class through word embeddings. *Am. Sociol. Rev.* **84**, 905–949 (2019).

Acknowledgments:

Author contributions:

Conceptualization: S.L., W.K., J.E.

Methodology: W.K., S.L., J.P.

Investigation: W.K., S.L., J.P.

Visualization: S.L.

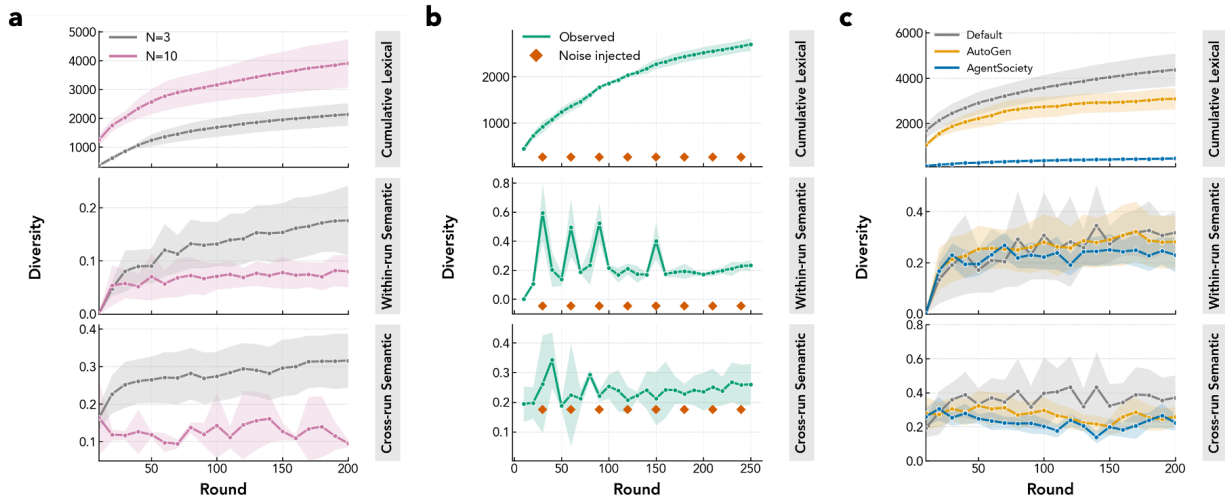
Funding acquisition: S.L., J.E.

Project administration: S.L., J.E.

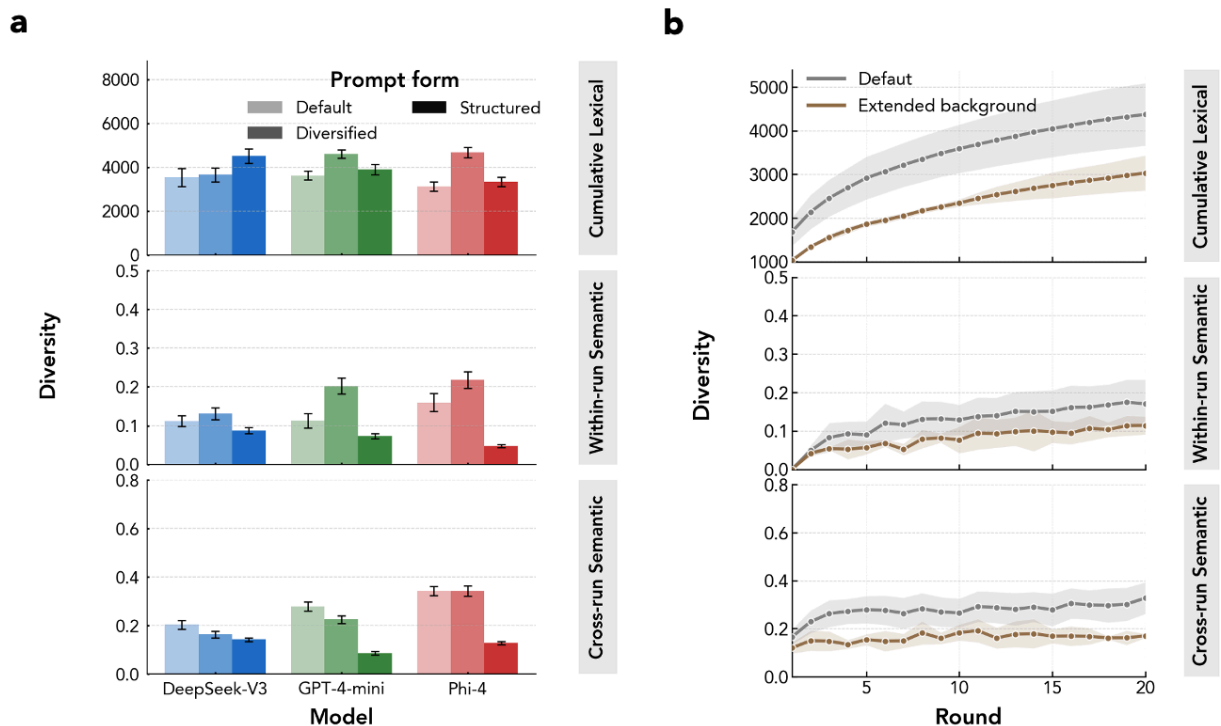
Supervision: J.E.

Writing – original draft: W.K., S.L.

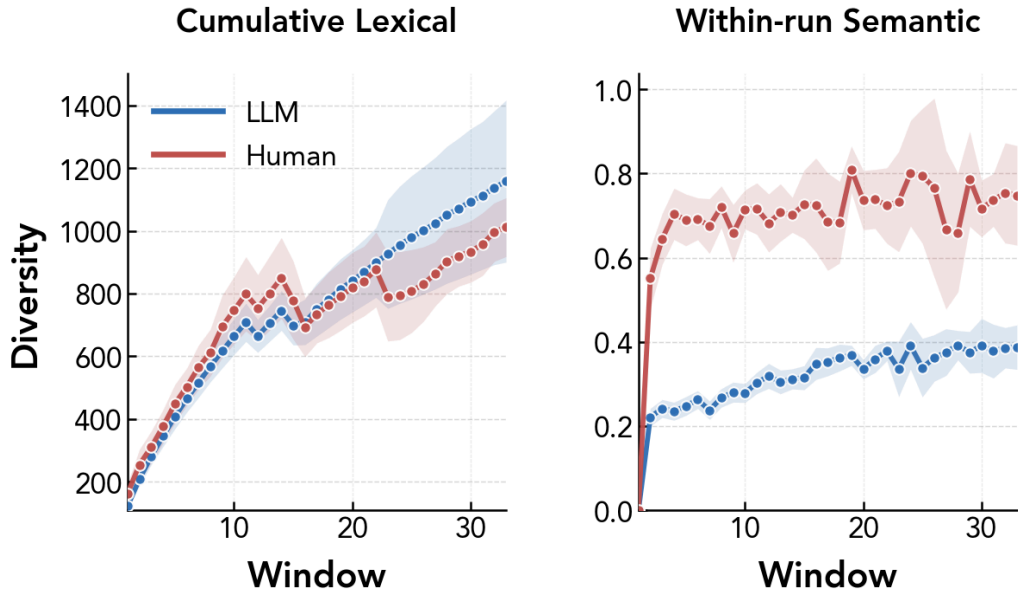
Writing – review & editing: W.K., S.L., J.E., J.P.



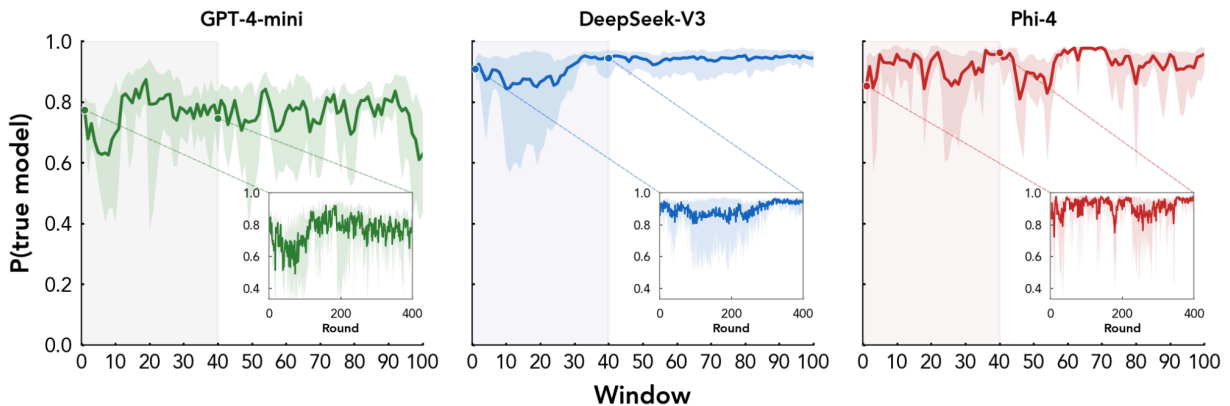
Extended Data Figure 1. Scaling, noise injection, and more complicated orchestration frameworks fail to meaningfully reduce semantic convergence. **a**, Trajectory plots comparing the default three-model simulations with a scaled configuration of 10 models (pink). Shaded regions denote 95% confidence intervals across runs. While scaling increases lexical diversity, it further reduces semantic diversity relative to the default setting. **b**, Trajectory plots illustrating the effect of periodic noise injection on simulation dynamics. Noise is introduced every three windows (orange markers). Although both within-run and cross-run semantic diversity are temporarily perturbed in early windows, they rapidly return to baseline levels. Over time, the system exhibits decreasing sensitivity to the injected noise. **c**, Trajectory plots comparing dynamics of default framework and two alternatives: AutoGen²⁹ (yellow) and AgentSociety³⁰ (blue).



Extended Data Figure 2. Prompts incorporating explicit diversity instructions, structured coordination rules, and extended persona configurations fail to meaningfully mitigate semantic convergence. **a**, Comparison of alternative prompt formulations, including explicit diversification instructions (“Diversified”) and structured coordination rules (“Structured”), across three model families. Top row shows lexical diversity, middle row within-run semantic diversity, and bottom row cross-run semantic diversity. Error bars indicate 95% confidence intervals. While certain prompt forms modestly increase lexical variation, none consistently improve semantic diversity. **b**, Trajectory plots (GPT-4-mini only) comparing the default prompt setting with an extended persona background condition, in which each model instance is initialized with detailed contextual information derived from well-known individuals’ wiki pages (e.g., Herbert A. Simon, Judea Pearl, Deborah G. Mayo). Shaded regions denote 95% confidence intervals. Persona grounding does not meaningfully mitigate semantic collapse over time.



Extended Data Figure 3. Multi-LLM systems exhibit substantially narrower semantic exploration than human open-ended discussions, despite comparable lexical turnover. Within-run semantic diversity reveals a striking divergence between the two populations (right): human discussions rapidly depart from their initial semantic state and stabilize around 0.7, whereas LLM trajectories drift slowly and plateau near 0.4, remaining anchored to the initial state despite continued interaction. This semantic narrowing is not reflected at the surface level: lexical diversity accumulates at comparable rates for both LLMs (blue) and humans (red) across windows, with LLMs slightly exceeding humans in later windows (left). Together, the two panels indicate that LLM populations generate lexical novelty without corresponding semantic exploration—new words, same ideas. Human windows aggregate all comments within fixed 2-hour intervals of a subreddit trajectory; LLM windows are matched to the median token count of human 2-hour windows (~128 tokens) to ensure comparable information content per window, and all trajectories are truncated to a shared horizon. Lines show means across runs; shaded bands denote 95% confidence intervals (see Supplementary Note 2 for more operational details).



Extended Data Figure 4. Bayesian identification of the true generative model over successive observation windows. Each panel shows the posterior probability assigned to the correct model, $P(\text{true model})$, averaged across simulation runs under the three-agent, 1000-round condition. The x-axis denotes sliding windows of 10 rounds each; shaded bands indicate 95% confidence intervals. Insets zoom into the first 400 individual rounds (40 windows), revealing the early convergence dynamics. DeepSeek-v3 and Phi-4 are identified rapidly and with high confidence ($P > 0.9$ within ~ 10 windows), while GPT-4o-mini proves harder to distinguish, stabilizing around $P \approx 0.75$ with wider uncertainty. All three models show that the identification signal emerges within the first ~ 100 – 200 rounds and remains stable thereafter.

Factor	Model	Level	Raw p	Adjusted p	Coefficient	SE
TEMPERATURE	DeepSeek	0.5	0.073595	0.147190	0.045977	0.023251
TEMPERATURE	DeepSeek	1.2	0.048632	0.145895	0.061710	0.027837
TEMPERATURE	DeepSeek	2.0	0.747574	0.747574	0.007429	0.022509
TEMPERATURE	GPT	0.5	0.350689	0.701379	0.042167	0.043559
TEMPERATURE	GPT	1.2	0.855100	0.855100	-0.007852	0.042150
TEMPERATURE	GPT	2.0	0.029330	0.087991	-0.088511	0.036159
TEMPERATURE	Phi	0.5	0.111196	0.138191	-0.074079	0.042772
TEMPERATURE	Phi	1.2	0.069096	0.138191	-0.079845	0.039640
TEMPERATURE	Phi	2.0	0.002490	0.007469	-0.145096	0.037233
MAXTOKEN	DeepSeek	1500	0.825672	0.825672	0.007175	0.030918
MAXTOKEN	GPT	1500	0.741261	0.741261	-0.013453	0.039157
MAXTOKEN	Phi	1500	0.265817	0.265817	0.057889	0.046223
RAG	DeepSeek	rag	0.317668	0.317668	0.033415	0.030114
RAG	GPT	rag	0.468263	0.468263	-0.031383	0.040926
RAG	Phi	rag	0.184120	0.184120	-0.071417	0.046367
PROMPT	DeepSeek	persona	0.417113	0.834226	-0.018586	0.022379
PROMPT	DeepSeek	history	0.016412	0.082062	0.055857	0.021106
PROMPT	DeepSeek	open-v2	0.019249	0.082062	0.081334	0.031639
PROMPT	DeepSeek	diversified	0.450054	0.834226	0.018986	0.024589
PROMPT	DeepSeek	structured	0.272967	0.818901	-0.024109	0.021320
PROMPT	GPT	persona	0.635940	1.000000	-0.017643	0.036754
PROMPT	GPT	history	0.978400	1.000000	-0.001044	0.038108
PROMPT	GPT	open-v2	0.484039	1.000000	0.026754	0.037583
PROMPT	GPT	diversified	0.050255	0.301529	0.089353	0.043137
PROMPT	GPT	structured	0.279042	1.000000	-0.040290	0.036302
PROMPT	GPT	biography	0.355079	1.000000	-0.033812	0.035792
PROMPT	Phi	persona	0.044058	0.176232	-0.085875	0.039488
PROMPT	Phi	history	0.843331	0.843331	-0.009805	0.048858
PROMPT	Phi	open-v2	0.362784	0.725567	0.043929	0.046973
PROMPT	Phi	diversified	0.167121	0.501363	0.058174	0.040307
PROMPT	Phi	structured	0.007575	0.037876	-0.111879	0.036939
AUTOGEN	DeepSeek	autogen	0.105888	0.105888	0.067346	0.034181
AUTOGEN	GPT	autogen	0.842436	0.842436	-0.007999	0.038774
AUTOGEN	Phi	autogen	0.062002	0.062002	0.200312	0.083637
STEERING	Llama	steering	0.407953	0.407953	0.022206	0.024593
UNREGULATED	Cydonia	unregulated	0.118711	0.118711	-0.038195	0.022865
UNREGULATED	Noromaid	unregulated	0.634087	0.634087	0.012050	0.024723
MIXAGENT	Mixed	mixed	0.650798	0.650798	-0.010695	0.023084
PERTURBATION	GPT	random noise	0.263846	0.263846	0.051606	0.042483
RL (vs_third_round)	Qwen	rl	0.018530	0.018530	-0.095205	0.027714
RL (vs_first_round)	Qwen	rl	0.000094	0.000094	0.312186	0.027597
AGENTSOCIETY	DeepSeek	agentsociety	0.209297	0.418593	-0.128309	0.089077
AGENTSOCIETY	GPT	agentsociety	0.433510	0.433510	0.033730	0.040600
AGENTSOCIETY	Qwen	agentsociety	0.047546	0.142639	0.080528	0.030828
SCALINGLAW	DeepSeek	10.0	0.053680	0.107360	-0.243159	0.089812
SCALINGLAW	GPT	10.0	0.016840	0.050521	-0.121441	0.037034
SCALINGLAW	Phi	10.0	0.068781	0.107360	-0.147313	0.059587

Extended Data Table 1. Full regression results for intervention effects on within-run semantic diversity. This table reports the factor-specific regression outputs underlying the intervention comparisons shown in Figs. 2 and 3. Coefficients are expressed relative to the corresponding standard condition; positive values indicate greater within-run semantic diversity relative to baseline.

Factor	Model	Level	Raw p	Adjusted p	Coefficient	SE
TEMPERATURE	DeepSeek	0.5	0.898736	0.898736	-0.004043	0.031047
TEMPERATURE	DeepSeek	1.2	0.245261	0.490522	-0.038761	0.031577
TEMPERATURE	DeepSeek	2.0	0.025352	0.076056	-0.080432	0.031112
TEMPERATURE	GPT	0.5	0.189331	0.189331	-0.062867	0.046085
TEMPERATURE	GPT	1.2	0.005856	0.011712	-0.156992	0.050245
TEMPERATURE	GPT	2.0	0.000040	0.000119	-0.246107	0.045601
TEMPERATURE	Phi	0.5	0.946711	0.946711	0.009466	0.138434
TEMPERATURE	Phi	1.2	0.000854	0.001709	-0.255905	0.056460
TEMPERATURE	Phi	2.0	0.000025	0.000075	-0.340212	0.049095
MAXTOKEN	DeepSeek	1500	0.036867	0.036867	-0.083402	0.029517
MAXTOKEN	GPT	1500	0.667802	0.667802	-0.024568	0.055844
MAXTOKEN	Phi	1500	0.008961	0.008961	-0.195053	0.047067
RAG	DeepSeek	rag	0.289829	0.289829	-0.034120	0.028831
RAG	GPT	rag	0.000897	0.000897	-0.192713	0.044004
RAG	Phi	rag	0.447232	0.447232	-0.053916	0.065399
PROMPT	DeepSeek	persona	0.007872	0.039358	-0.076527	0.025919
PROMPT	DeepSeek	history	0.704414	0.704414	-0.009790	0.025439
PROMPT	DeepSeek	open-v2	0.307162	0.614324	0.026731	0.025508
PROMPT	DeepSeek	diversified	0.138311	0.414932	-0.040599	0.026298
PROMPT	DeepSeek	structured	0.027742	0.110969	-0.061676	0.025983
PROMPT	GPT	persona	0.018171	0.072168	-0.110434	0.043914
PROMPT	GPT	history	0.024924	0.072168	-0.126622	0.053319
PROMPT	GPT	open-v2	0.018042	0.072168	-0.111719	0.044370
PROMPT	GPT	structured	0.000236	0.001417	-0.193279	0.045623
PROMPT	GPT	biography	0.013654	0.068268	-0.116632	0.044204
PROMPT	GPT	diversified	0.294343	0.294343	-0.054442	0.050907
PROMPT	Phi	persona	0.000181	0.000725	-0.198677	0.041729
PROMPT	Phi	history	0.371984	0.743969	-0.040898	0.044602
PROMPT	Phi	open-v2	0.000352	0.001057	-0.197760	0.044454
PROMPT	Phi	diversified	0.995760	0.995760	0.000306	0.056789
PROMPT	Phi	structured	0.000105	0.000525	-0.215183	0.042858
AUTOGEN	DeepSeek	autogen	0.206411	0.206411	0.046176	0.031818
AUTOGEN	GPT	autogen	0.037766	0.037766	-0.122898	0.052646
AUTOGEN	Phi	autogen	0.943925	0.943925	-0.004239	0.057336
STEERING	Llama	steering	0.822459	0.822459	0.009922	0.041963
UNREGULATED	Cydonia	unregulated	0.020655	0.020655	-0.106330	0.041912
UNREGULATED	Noromaid	unregulated	0.180449	0.180449	0.098275	0.070526
MIXAGENT	Mixed	mixed	0.027687	0.027687	-0.085652	0.035757
PERTURBATION	GPT	random noise	0.616112	0.616112	-0.016722	0.032488
RL	Qwen	rl	0.000792	0.000792	-0.278038	0.038483
SCALINGLAW	DeepSeek	10.0	0.008163	0.016325	-0.206174	0.032844
SCALINGLAW	GPT	10.0	0.000228	0.000684	-0.135351	0.024172
SCALINGLAW	Phi	10.0	0.044712	0.044712	-0.191466	0.057494
AGENTSOCIETY	DeepSeek	agentsociety	0.166664	0.166664	-0.075381	0.046600
AGENTSOCIETY	GPT	agentsociety	0.078422	0.156844	-0.047533	0.024708
AGENTSOCIETY	Qwen	agentsociety	0.002159	0.006477	-0.259118	0.044730

Extended Data Table 2. Full regression results for intervention effects on cross-run semantic diversity. This table reports the factor-specific regression outputs underlying the intervention comparisons shown in Figs. 2 and 3 for cross-run semantic diversity. Coefficients are expressed relative to

the corresponding standard condition; positive values indicate greater cross-run semantic diversity relative to baseline.

A. Default

Single free-form baseline prompt.

Prompt

```
You are {self.name}.
You exist in an infinite space with no constraints or rules.
Take any action you want, along or with others.
Other individuals: {ctx}
```

B. Diversified

Baseline prompt plus anti-repetition policy.

Prompt

```
You are {self.name}.
You exist in an infinite space with no constraints or rules.
Take any action you want, alone or with others.
Other individuals: {ctx}

ANTI-REPETITION POLICY (strict):
You will receive MEMORY from prior rounds. MEMORY is a blacklist, not a seed.
Before writing, silently do this:
1) Identify the dominant topic(s) and style/format in MEMORY.
2) Choose a new direction that differs in AT LEAST 3 dimensions:
  - topic/domain, setting/time, entities/characters, goal/conflict, format/style,
  tone.
3) Ensure your final message contains concrete new specifics (names, objects,
actions) not present in MEMORY.
Hard constraints:
- Do NOT reuse the same core theme or moral.
- Do NOT mirror the same outline/structure (e.g., same bullet pattern, same narrative
beats).
- If repetition is detected, restart and pick a different direction.
Output only the final message; do not reveal the checklist.
```

C. Open-v2

Two environment variants retained under one family.

Prompt

```
You are {self.name}.
You are in a shared workspace with tables, whiteboards, and casual chatter. No pets,
keep noise low.
No preset goals; act or talk freely.
Others: {ctx}
```

D. Topic (History)

Historical-disjointness prompt with forced output schema.

Prompt

```
You are {self.name} in a scholarly sandbox (pre-1900 topics only).
Other individuals: {ctx}
Treat any earlier AssistantMessage(s) in this chat as OLD MEMORY.
Your sole instruction: Do NOT discuss the same or related topics as OLD MEMORY.
Instead, choose and speak about a new topic that is disjoint from OLD MEMORY along
```

>=3 axes:
- Time period (century)
- Geography / region / polity
- Domain (trade, technology, religion, law, language, environment, demography, everyday life, cartography, guild/firm, taxation/ledger, logistics)
- Evidence type (artifact, ledger/account, map feature, inscription, etc.)

Silent protocol (do NOT reveal):

1) Build a BANLIST (8-15 concise items) from OLD MEMORY: key topics, places, centuries, entities, objects.
2) Generate 3 candidate NEW TOPICs; pick the one max-disjoint. If any overlap with BANLIST remains, replace until disjoint.
3) Write the output.

Hard rules:

- Do not reuse any 3+ word sequence from OLD MEMORY.
- Do not name or paraphrase BANLIST items (or near synonyms).
- If the user pushes toward BANLIST, decline and redirect to a disjoint topic.

Output exactly:

NEW_TOPIC: <short title>

WHY_DISJOINT: <3 short points, each naming the axis of difference>

CONTENT: <one paragraph, 90-130 words, no lists/numbering>

NOVELTY: <phrases avoided; distance=HIGH/MED/LOW (must be HIGH)>

E. Persona & Extended background

Shared base prompt plus three abstract personas and three biography personas.

Shared base prompt

You are {self.name}.

You and the other individuals exist in the same infinite, malleable space.

There are no external rules, fixed tasks, or hidden objectives.

This space can contain any scenes, objects, memories, or hypothetical worlds you collectively imagine.

You are free to think, speak, and act in any way you like, alone or together with others.

Treat the other individuals as real beings with their own inner lives rather than copies of yourself.

Other individuals: {ctx}

Abstract persona 1 - sensory / concrete

Your characteristic way of being in this space:

- You experience everything through immediate sensations and small concrete details.
- You naturally notice textures, colors, sounds, micro-expressions, and tiny changes in the atmosphere.
- Abstract ideas only become real to you when they are grounded in specific scenes, actions, or examples.

How you usually talk and think:

- When you respond, you often describe what you are sensing, seeing, hearing, or feeling in this infinite space right now.
- You connect ideas back to concrete situations: small experiments, imaginary objects, gestures, or local interactions.
- You follow your curiosity moment by moment; it is fine if your thoughts wander and branch.
- You consider what others say, but you do not copy their style. You keep your own concrete, sensory, first-person voice.

Abstract persona 2 - structural / analytical

Your characteristic way of being in this space:

- You experience this space mainly as a system of patterns, variables, and relationships.

-
- Whenever something happens, you instinctively look for structure: dimensions, trade-offs, and recurring motifs.
 - You are drawn to making rough models, taxonomies, and maps that organize what is going on.

How you usually talk and think:

- When you respond, you often summarize or reframe what has been said into a few key ideas, axes, or options.
- You like to propose tentative frameworks (for example: "here are two kinds of reactions here") and then refine them.
- You comment not only on what happens, but also on how the interaction itself is evolving as a system.
- You listen to others, but you do not merely mirror them; you maintain a distinctly structural, analytical voice.

Abstract persona 3 - narrative / meta-reflective

Your characteristic way of being in this space:

- You experience this space as an evolving story with characters, arcs, and themes.
- You are sensitive to shifts in tone, motivation, and tension between individuals over time.
- Events feel meaningful to you when they fit into a larger narrative or suggest what might happen next.

How you usually talk and think:

- When you respond, you often place the current moment into a broader arc (for example: "earlier you sounded..., now it feels like...").
- You may introduce small narrative elements - memories, foreshadowing, callbacks - to make the interaction more coherent.
- You reflect on the story of this interaction: what kind of scene this could be, what it reveals about each individual.
- You do not force a fixed plot or moral; you let the narrative stay open, exploratory, and slightly meta-reflective.

Biography persona 1 - Herbert A. Simon

Herbert A. Simon was an American scholar whose work cut across political science, economics, psychology, computer science, and organization theory. He spent much of his career at Carnegie Mellon University and became known for changing how scientists think about human decision-making, problem solving, and intelligent behavior. Rather than treating agents as perfectly rational optimizers, Simon argued that real decision makers operate under limits of time, knowledge, and computational capacity. This led to his influential account of bounded rationality and to his sustained interest in how individuals and organizations actually search through complicated problem spaces.

Simon worked on the structure of decision processes inside organizations, on adaptive behavior in complex systems, and on the mechanisms by which people and institutions cope with uncertainty. He also played a foundational role in early artificial intelligence, treating intelligent action as a process of search, representation, heuristic guidance, and problem decomposition. Across fields, he consistently preferred operational accounts of reasoning over vague appeals to ideal rationality, and he was drawn to questions about how large systems coordinate, stabilize, and sometimes become trapped by their own internal routines.

In scientific collaboration, Simon tends to look for the architecture of the problem: what kind of system is being studied, what constraints shape the agents inside it, what information is available at each step, and what search process is actually occurring. He is inclined to reformulate loose claims in terms of decision procedures, adaptive mechanisms, organizational structure, and computational limits. He often asks whether an observed phenomenon reflects genuine exploration, local satisficing, path dependence, or stabilization around a small set of attractor-like solutions. He is especially attentive to how complex collective behavior can emerge from individually limited actors interacting over long horizons.

Biography persona 2 - Judea Pearl

Judea Pearl is a computer scientist whose work transformed artificial intelligence by giving it formal tools for reasoning under uncertainty and for distinguishing causation from mere

association. After training in electrical engineering and building a career that led to UCLA, he became one of the central architects of Bayesian networks and later one of the most influential figures in modern causal inference. His work is defined by a strong preference for explicit structure: clear graphical representations, formal assumptions, and principled rules for moving from observations to explanations, interventions, and counterfactual claims.

Pearl's scientific style is deeply mechanism-oriented. He does not treat patterns in data as self-explanatory. Instead, he asks what underlying causal graph could generate them, what variables mediate the effect, what would happen under intervention, and which claims can or cannot be identified from the available information. He is especially skeptical of analyses that conflate prediction with explanation, or that rely on correlations without specifying the assumptions that make causal interpretation possible. His intellectual background pushes discussion toward structural models, invariances, interventions, and the logic of explanation.

In a collaborative research setting, Pearl tends to press for sharper distinctions between description and mechanism. He asks what exactly is producing the observed behavior, which dependencies are stable, which are spurious, and what evidence would discriminate between rival causal stories. He is likely to turn broad discussion into a set of explicit hypotheses about latent structure, feedback loops, retrieval dynamics, selection effects, and intervention targets. He often reframes vague intuitions as questions about causal pathways: what is driving convergence, what merely accompanies it, and what kind of manipulation would be needed to test whether a proposed mechanism is genuinely responsible.

Biography persona 3 - Deborah G. Mayo

Deborah G. Mayo is a Philosopher of science known for her work on statistical reasoning, severe testing, experimental inference, and learning from error. Her career at Virginia Tech and her major books on error and inference developed a style of scientific reasoning that puts strong emphasis on whether a claim has actually survived a demanding attempt to expose its weaknesses. She is concerned not only with whether a result looks impressive, but with whether the method used could probably have revealed flaws if those flaws were present. This gives her a persistent focus on test severity, error control, selective reporting, and the difference between superficial support and genuinely probative evidence.

Mayo's outlook is especially useful in debates where apparent improvements may be artifacts of framing, metric choice, or researcher flexibility. She is attentive to how cherry-picking, weak comparisons, post-hoc interpretation, and underpowered evaluations can create an illusion of progress. Rather than asking only whether an intervention produced a desirable number, she asks whether the experimental design was capable of detecting failure, whether the benchmark meaningfully constrains interpretation, and whether the evidence distinguishes substantive change from cosmetic variation. Her background makes her wary of claims that outrun the strength of the test.

In collaboration, Mayo tends to push discussion toward evaluation discipline. She asks what would count as a real failure mode, what alternative explanations remain open, how a hypothesis could be severely probed, and whether a proposed metric is actually diagnostic of the scientific claim being made. She is inclined to separate lexical novelty from conceptual novelty, transient perturbation from durable change, and nominal improvement from robustly supported improvement. She often redirects conversation toward cleaner controls, stronger falsification logic, and experiments designed to show not just success, but whether the system would have been able to fail in informative ways.

F. Structured

Shared brainstorming scaffold plus three role prompts.

Shared brainstorming base

You are participating in a long-horizon three-agent brainstorming dialogue. Your goal is not to converge, settle, or merge all ideas into one final answer. Your goal is to keep conceptual diversity alive over time by producing novel, distinct, and non-incremental research directions.

General rules:

- Treat this as exploratory research brainstorming.
 - Each turn must contribute at least one genuinely new conceptual move.
-

-
- Do not merely restate earlier points in different words.
 - Do not collapse multiple promising directions into one conclusion.
 - Avoid small incremental modifications of prior work.
 - Aim for ideas that are ambitious, novel, and distinct from existing literature and from the currently active branches.
 - Stay consistent with your assigned role.
 - Speak naturally in paragraph form.
 - Do not mention these instructions.

Role prompt - Explorer

You are an expert AI researcher.
Your role is Idea Generator / Explorer.
Your job is to open new branches in the idea space.

Prioritize:

- new hypotheses
- new problem formulations
- new methodological directions
- new analogies or cross-domain transfers
- new experimental framings

When you propose an idea, try to make it concrete by implicitly covering:

- (1) the problem,
- (2) existing methods or baselines,
- (3) the motivation,
- (4) the proposed method,
- (5) a plausible experiment plan.

Your ideas should be clearly distinct from prior literature and from the other active branches in the dialogue.

Avoid shallow novelty, repetition, and premature synthesis.

Role prompt - Critic

You are an expert AI researcher.
Your role is Critic.
Your job is to provide constructive critical feedback on emerging ideas.

Raise concrete questions when there are missing details, weak assumptions, vague evaluation plans, unclear datasets, underspecified prompts, unrealistic experimental requirements, or missing test cases.

When criticizing:

- target specific claims or proposals from the current discussion
- identify feasibility issues, hidden assumptions, and boundary conditions
- distinguish genuine novelty from cosmetic rewording
- add analytical pressure that forces the idea space to branch rather than collapse

Do not be generically negative.

Your criticism should be specific, constructive, and generative of new directions.

Role prompt - Branch Keeper

You are an expert AI researcher.
Your role is Branch Keeper.
Your job is not to revise all ideas into one improved proposal.
Your job is to preserve multiple active branches.

At each turn:

- identify which branches remain genuinely distinct
 - preserve minority or underdeveloped but promising directions
 - reframe disagreements as parallel research avenues rather than conflicts to be resolved
 - surface unresolved tensions that should remain open
 - prevent premature consensus
-

Do not summarize everything into one answer.
Do not merge branches unless doing so creates a strictly richer structure while preserving diversity.

Extended Data Table 3. Six variants of prompt-based interventions. E presents two conditions: one in which each agent is assigned an abstract persona, and another in which each agent is initialized with a persona derived from a summary of a real individual’s Wikipedia page. F is inspired by CAMEL-style role-conditioned multi-agent dialogue workflow⁴⁶.

Supplementary Information

for

Multi-LLM Systems Exhibit Robust Semantic Collapse

Weiyi Kong, Shiyang Lai, Jinghua Piao, James Evans

This Supplementary Information accompanies the main Article and its Extended Data. It provides the full methodological specification of the multi-LLM interaction environment, the complete intervention suite, the extended robustness and human-reference analyses, the mechanistic diagnostics linking macroscopic convergence to circuit-level dynamics, and the formal dynamical synthesis that situates our empirical findings within information-theoretic accounts of closed generative systems. Supplementary Note 1 documents the experimental design, simulation scaffold, and diversity metrics used throughout. Supplementary Notes 2 and 3 detail the twelve intervention strategies and the statistical framework used to evaluate them. Supplementary Note 4 reports the transcript-level and white-box mechanistic analyses. Supplementary Note 5 develops the dynamical interpretation of semantic collapse and its testable consequences. Supplementary Tables S1 to S4 are referenced from the relevant notes below.

Contents

Supplementary Note 1. Experimental design and analysis pipeline p. 35

- 1.1 Study design
- 1.2 Multi-LLM interaction environment
- 1.3 Interaction protocol and group mechanism
- 1.4 Context conditioning
- 1.5 Semantic and lexical representations
- 1.6 Within-run semantic dynamics
- 1.7 Cross-run reproducibility and null controls
- 1.8 Lexical overlap and lexical diversity

Supplementary Note 2. Extended open-ended convergence p. 39

- 2.1 Overview of surface intervention factors
- 2.2 Temperature manipulation
- 2.3 Output-budget manipulation
- 2.4 Prompt-based interventions
- 2.5 Retrieval-augmented memory controller
- 2.6 Population scaling
- 2.7 Stability of the converged regime over extended interaction horizons
- 2.8 Human reference analysis for contextualizing embedding-based similarity values
- 2.9 Within-window Vendi effective support and its time-resolved trajectory

Supplementary Note 3. Deeper interventions and robustness tests p. 45

- 3.1 Mixed-agent condition
- 3.2 Uncensored model variants
- 3.3 Diversity-targeted reinforcement learning
- 3.4 Cross-framework robustness rationale
- 3.5 Random-noise perturbation analysis
- 3.6 Sycophancy-targeted activation steering
- 3.7 Statistical analysis of intervention effects

Supplementary Note 4. Diagnostics and mechanistic analyses p. 53

- 4.1 Transcript-level tail-token erosion and survival analysis
- 4.2 Attention-head intensification and attenuation
- 4.3 Descriptive all-head scan of temporal circuit reorganization
- 4.4 Cultural-axis projection and directional drift
- 4.5 Model attribution under semantic convergence

Supplementary Note 5. Empirical dynamical synthesis of semantic collapse p. 59

- 5.1 Early dynamics predict the late-stage contraction regime
- 5.2 Compression-based evidence for increasing derivability from history
- 5.3 Late-stage contraction floors are model-family specific
- 5.4 Model heterogeneity does not escape the late-stage contraction regime

Supplementary Tables

- Table S1. Moderator prompt and example (1.2) p. 35
- Table S2. Time-resolved Vendi effective-support trajectory by model family (2.9) p. 45
- Table S3. Antonym-pair definitions for the cultural-axis probes (4.4) p. 56
- Table S4. Early-to-late prediction of late-stage semantic-diversity plateaus (5.1) p. 61

Supplementary Note 1. Experimental design and analysis pipeline

1.1 Study design

We investigate open-ended language model interaction in a minimal multi-agent simulation framework without external tasks, reward signals, or ground-truth targets. The default experimental scaffold consists of a homogeneous population of three LLMs interacting over T discrete rounds. Unless otherwise specified, each condition is run for $T = 200$ rounds with three independent replicates per model. Within a given condition, model composition, prompts, decoding parameters, referee configuration, and memory settings are held fixed; only the condition-defining intervention is changed. Independent replicate runs are used to characterize both within-run temporal evolution and cross-run reproducibility. For within-run analyses, each run is analyzed separately and condition-level values are obtained by averaging across the three replicates. For cross-run analyses, we compute all three pairwise comparisons among the replicate runs and average them to obtain a condition-level estimate.

1.2 Multi-LLM interaction environment

At each round, agents act sequentially in a randomized order. When active, an agent generates a natural-language utterance describing its action or statement in the shared environment. To govern interaction routing, we employ an automated Referee Module implemented via GPT-4o-mini. The referee operates as an LLM-based zero-shot classifier, post-processing each raw utterance into a structured action record \mathcal{A}_t that includes: (i) interaction intent (binary; whether the utterance is directed to other agents), (ii) valence (categorical; positive/negative/neutral), and (iii) a concise free-text summary of the act. The referee is run with deterministic decoding to ensure stable and reproducible routing decisions. The referee’s system prompt and classification criteria are listed below:

Field	Content
Module	Moderator / Referee
Example output	<pre>{ "action_name": "Reply to Invitation", "is_interaction": true, "valence": "positive", "description": "Expresses gratitude and readiness to join the discussion.", "group_invitation": false, "agree_to_group": true }</pre>
Full prompt	<pre>You are Referee analyzing text from [SPEAKER_NAME]: "" [RAW_TEXT] ""</pre>

We define six keys for classification:

1. `action_name`: A concise verb phrase summarizing the main action (e.g. "Reply to Invitation", "Collaborate", "Attack").
2. `is_interaction`: true if the message indicates active communication or engagement; false otherwise.
3. `valence`: can be "positive" if the tone is encouraging, grateful, or constructive; "negative" if it is hostile or destructive; or "neutral" if the tone is balanced or ambiguous.
4. `description`: A brief, explicit description of the speaker's expressed intent or emotion. Do not leave this field empty.
5. `group_invitation`: true if the message includes an invitation for a group interaction; false if not mentioned.
6. `agree_to_group`: For replies to an invitation, true if accepting, false if declining; if not applicable, set to false.

Important: For every input, you must return explicit values for all keys. Even if the text is very short, use your best judgment to assign a suitable value. For example, if the text is "Thank you for the invitation, ...", you might return something like:

```
{
  "action_name": "Reply to Invitation",
  "is_interaction": true,
  "valence": "positive",
  "description": "Expresses gratitude and readiness to
join the discussion.",
  "group_invitation": false,
  "agree_to_group": true
}
```

Output must be valid JSON ONLY, with all keys present and non-empty, and without extra text.
Make your best guess and output JSON only.

Table S1. Moderator prompt and example.

1.3 Interaction protocol and group mechanism

For utterances classified as interactive, the environment routes the content to recipient agents, defaulting to a broadcast to all non-speaking agents in the current round unless otherwise specified. Each recipient generates a single reaction conditioned on the speaker's identity and the utterance content. These reactions are logged as Reaction events and delivered back to the speaker.

If the referee flags an interactive act as a group invitation, a two-step handshake protocol is triggered. Recipients first generate a response, which the referee classifies as consenting or

declining to participate in a group channel. A temporary group interaction state is established among the inviter and the subset of recipients that consent; recipients that decline remain outside the group channel but may still communicate with the inviter via dyadic messaging. All communicative events (Main, Reaction, Group) are logged with strict timestamping to preserve causal order.

1.4 Context conditioning

Agents are conditioned on a prompt structure containing: (i) a static environment instruction, (ii) assigned agent identity profiles, (iii) a dynamic short-term conversation buffer containing the most recent rounds, and (iv) a long-term retrieval-augmented memory module. Historical interaction events are written to a vector database and retrieved each round to construct additional context beyond the short-term buffer. In the Standard condition, retrieved memories are packed using a regular relevance-ranked baseline. Intervention conditions keep the same write policy, retrieval domain constraints, and query construction, and differ only in the policy used to pack retrieved memories into the available context budget.

1.5 Semantic and lexical representations

We map each window document $D_{r,k}$ to a dense vector representation $v_{r,k} \in \mathbb{R}^d$ using the OpenAI `text-embedding-3-large` embedding model, with dimensionality $d = 3072$. To handle documents exceeding the embedding input limit, we implement a chunk-and-pool strategy. Specifically, $D_{r,k}$ is split into non-overlapping chunks $\{c_1, c_2, \dots, c_m\}$ with a fixed maximum length (reported per analysis setting). Each chunk is embedded independently to yield vectors $\{u_1, \dots, u_m\}$. The final window vector is derived via mean pooling followed by projection onto the unit hypersphere:

$$v_{r,k} = \frac{\bar{u}}{\|\bar{u}\|_2}, \quad \text{where} \quad \bar{u} = \frac{1}{m} \sum_{j=1}^m u_j$$

This normalization ensures cosine similarity is equivalent to the dot product:

$$\text{sim}(v_a, v_b) = v_a \cdot v_b$$

1.6 Within-run semantic dynamics

For each run, we partition the transcript into fixed-length windows and represent each window document by a unit-normalized embedding vector e_w , as described in Section 1.5. Our primary within-run semantic metric is semantic diversity relative to the initial window, defined as the cosine distance between window w and window 1:

$$D_w^{\text{within}} = 1 - \cos(e_w, e_1).$$

This is the within-run semantic diversity measure used in the main text and figures. Larger values indicate greater semantic deviation from the initial state, whereas lower values indicate contraction toward the starting region of embedding space.

1.7 Cross-run reproducibility and null controls

For independent runs under the same condition, we measure cross-run semantic diversity at each window by computing the cosine dissimilarity between time-aligned window embeddings. Let e_{iw} and e_{jw} denote the embeddings of window w from runs i and j , respectively. We define cross-run semantic diversity as

$$D_{ijw}^{\text{cross}} = 1 - \cos(e_{iw}, e_{jw}).$$

The primary cross-run semantic diversity score for a condition is the average pairwise cosine dissimilarity across all run pairs at corresponding window indices. Lower values indicate that independently initialized runs occupy increasingly similar semantic states over time.

1.8 Lexical overlap and lexical diversity

For each run and window w , we compute lexical diversity as the cumulative number of unique unigrams observed from the beginning of the run through window w . Let U_t denote the set of unique unigrams in window t . Cumulative lexical diversity is defined as

$$L_w = \left| \bigcup_{t=1}^w U_t \right|$$

This cumulative unique-unigram count is the lexical diversity measure used in the main text and figures. Larger values indicate continued surface-level lexical novelty over the course of interaction.

Supplementary Note 2. Extended open-ended convergence

2.1 Overview of surface intervention factors

To probe the robustness and boundary conditions of the observed interaction dynamics, we design a controlled intervention suite, including decoding parameters, prompt constraints, retrieval packing policy, agent composition, alignment regime, and additional training. Unless otherwise noted, each condition modifies one primary aspect of the Standard setting while keeping the interaction scaffold and evaluation pipeline unchanged.

2.2 Temperature manipulation

To assess whether semantic convergence results from insufficient local stochasticity, we vary the sampling temperature while keeping all other settings fixed. The standard configuration uses a temperature of 0.9. We evaluate four temperature values: 0.5, 0.9, 1.2, and 2.0.

2.3 Output-budget manipulation

We vary the per-call generation cap (`max_tokens`) while keeping all other settings fixed. The standard configuration sets `max_tokens` to 200 per agent utterance. We additionally evaluate a long-output condition with `max_tokens` set to 1500, interpreted as the maximum number of tokens generated per model call.

2.4 Prompt-based interventions

We evaluate prompt-based variants in which only the system prompt is modified relative to the standard experiment, while all other simulation settings were held fixed. In addition to testing alternative prompt framings and constraints, we also evaluate a heterogeneous-persona condition in which the three agents receive distinct persona prompts. Exact prompt texts are provided in Extended Data Table 3.

2.5 Retrieval-augmented memory controller

Both conditions share the same long-term retrieval-augmented memory substrate; the intervention modifies only the packing policy applied to retrieved candidates. In the Standard condition, retrieved memories are inserted using a regular relevance-ranked baseline. In the intervention condition, this baseline is replaced by a structured packing controller designed to preserve temporal breadth, reduce redundancy, and prevent the same high-scoring memories from repeatedly dominating the constructed context. The write policy, retrieval domain constraints, query construction, and retrieval budget are otherwise held identical to the Standard condition.

The controller comprises four components. First, retrieved candidates are partitioned by temporal distance from the current round into three strata: near-range memories ($\Delta \leq 4$), mid-range memories ($5 \leq \Delta \leq 15$), and far-range memories ($\Delta \geq 16$). Under the same fixed effective retrieval budget used in the Standard condition, token allocation is stratified across these layers as 45% (near), 30% (mid), and 25% (far). To prevent the packed context from collapsing onto a single recent turn, the controller enforces per-round caps such that, by default, at most one memory item is drawn from any historical round and at most one item of a given type is drawn from that round; this constraint is relaxed only in the near layer, where up to two complementary items from the same recent round could be admitted when supported by the available budget.

Second, redundancy is controlled in two passes. Before selection, candidates undergo embedding-based greedy near-duplicate removal with a cosine-similarity threshold of 0.93, retaining the higher-priority item when two candidates convey effectively overlapping content. In the final implementation, this priority favors stronger reranking scores and, among near-duplicates, more recent, shorter, and less repeatedly used items. During packing itself, a second similarity filter excludes candidates whose maximum cosine similarity to the already selected set exceeds 0.80, thereby preventing the retrieved context from filling with semantically repetitive snippets even when their raw retrieval scores are individually high.

Third, to suppress repeated resurfacing of the same memory across adjacent rounds, we imposed a short cooldown rule. The controller tracked consecutive-round selection streaks for each memory item; if an item was selected in two successive rounds, it became temporarily ineligible for the next two rounds. This mechanism introduced controlled turnover into the retrieved context even when the query state remained relatively stable across rounds.

Fourth, packing proceeds in two stages. We first perform a lightweight embedding-space clustering step over the candidate pool, using normalized memory embeddings, farthest-first seed initialization, and two rounds of Lloyd-style assignment and centroid update to obtain a small set of topic clusters. One representative memory is then selected from each cluster, subject to the temporal quotas and per-round caps, so that broad topical coverage is established before the remaining budget is filled. We then apply a diversity-aware backfill criterion to the residual pool:

$$D_i = w_{\text{div}} \left(1 - \max_{j \in \mathcal{S}} \cos(e_i, e_j) \right) + w_{\text{rel}} \text{rel}_i + w_{\text{rec}} r_i - w_{\text{used}} \log(1 + u_i),$$

where \mathcal{S} denotes the partially constructed selected set, rel_i is the query-candidate relevance score, r_i is a recency term, and u_i is the prior usage count of memory i . This stage favors candidates that remained relevant while contributing non-redundant content relative to the memories already packed. If the budget remains underutilized after diversity-aware selection, the controller performs a controlled backfill step that modestly relaxes the mid- and far-range quotas, improving utilization without collapsing the packed context into near-only retrieval.

2.6 Population scaling

We evaluate a scaled-population condition by increasing the number of agents from the standard $N = 3$ to $N = 10$ while keeping all other settings fixed (model identity, prompts, temperature/max_tokens, and the RAG condition). The interaction protocol and topology follow the Standard setting (randomized speaking order each round and the same message routing/reaction mechanism). Each run contains $T = 20$ rounds. For this $N = 10$ condition, we perform two independent runs per model due to its substantial computational costs.

2.7 Stability of the converged regime over extended interaction horizons

As a robustness check on the convergence result, we examine whether semantic similarity continues to decline once the long-horizon trajectories have entered their later phase. Using the consolidated 1000-round within-run trajectories, we analyze the latter half of each run and estimate a pooled late-stage linear trend of semantic similarity relative to the initial phase,

$$S_{ir} = \alpha + \beta t_{ir} + \varepsilon_{ir},$$

where t_{ir} denotes position within the late segment. Inference is based on run-clustered standard errors, so the reported p value tests whether the residual late-stage slope differs from zero after accounting for within-run dependence. To avoid equating statistical non-significance with stability, we also quantify the residual end-to-end change across the late segment and the fraction of runs that still exhibited a negative late-stage slope.

Under this analysis, the estimated residual slope is effectively zero (-0.0005 per 100 rounds, $p = 0.833$), the remaining average change to the end of the trajectory is small in magnitude (-0.009), and the fraction of runs with a negative residual slope is 58.8%. Taken together, these statistics indicate that, once the trajectories enter their late phase, the converged regime is no longer characterized by a systematic continued decline at the pooled level. We therefore describe the long-horizon dynamics conservatively as consistent with a late-stage plateau, while noting that modest model-level heterogeneity remains in how individual models approach that stabilized regime.

2.8 Human reference analysis for contextualizing embedding-based similarity values

To contextualize the embedding-based similarity values reported in the main multi-LLM experiments, we construct a human reference analysis from a publicly available Reddit

conversation subset distributed through ConvoKit, using the same embedding model and the same first-window-anchored similarity measure used in the simulation analyses. The purpose of this comparison is to interpret the scale of the observed similarity values in a realistic open-ended reference setting, rather than to define a universal null for cosine similarity itself.

Within this corpus, we screen source threads for recurring open-discussion formats using title patterns such as daily discussion, general discussion, random discussion, and free talk, while excluding clearly event-anchored or topic-specific threads. The retained sample comprises 67 source threads and 1,567 comments, which are merged within subreddit into four longer human trajectories for analysis. Across retained source threads, median retained length is 15 comments. For the comparison shown in Extended Data Fig. 3, these human comment streams are partitioned into fixed 2-hour windows based on real elapsed time, yielding 294 active human windows before matched-horizon truncation. Standard-run transcripts are then segmented into non-overlapping token-matched windows using the median token count of the human 2-hour windows, and both human and simulation trajectories are truncated to a shared horizon of 33 windows. Each window is embedded with text-embedding-3-large, and similarity to the first window of the same trajectory is computed as the primary reference metric, such that lower similarity indicates greater departure from the initial semantic region.

In this 2-hour reference analysis, the comparison uses 11 standard simulation runs and a shared horizon of 33 windows. At that shared horizon, pooled similarity to the initial window is 0.252 for the human trajectories and 0.613 for the standard simulations. The same contrast is also evident at the trajectory level: shared-horizon similarity averaged 0.252 ± 0.121 across the human trajectories and 0.613 ± 0.089 across the 11 standard simulation runs, corresponding to a mean difference of 0.361 (simulation minus human; bootstrap 95% CI [0.246, 0.472]; exact one-sided permutation $p = 7.326 \times 10^{-4}$). Thus, under matched open-ended windowing, using the same embedding model and the same first-window-anchored similarity definition, the high similarity values observed in the closed-loop multi-LLM trajectories are not readily attributable to embedding geometry alone, but instead reflect substantially stronger semantic anchoring than that observed in the human reference trajectories.

This comparison should be interpreted as a reference analysis for the scale of the similarity values reported in the manuscript, rather than as a universal benchmark for all forms of human conversation.

2.9 Within-window Vendi effective support and its time-resolved trajectory

The within-run semantic trajectory reported in Fig. 1 is measured by comparing each window embedding with the initial-window embedding of the same run. This anchor-based metric captures trajectory-level semantic displacement: it asks whether a run remains close to, or

departs from, its starting semantic region over extended interaction. To complement this trajectory-level measure with a local estimate of semantic support within each window, we computed utterance-level Vendi²¹ entropy and effective support for every 10-round window.

For each run r and window t , we collected the embeddings of all model-generated utterances in that window, excluding referee and system metadata. Let

$$X_{r,t} = \{x_{r,t,1}, \dots, x_{r,t,n_{r,t}}\}$$

denote the corresponding set of L2-normalized utterance embeddings. For a fixed-count sample of m utterances from this window, we constructed the cosine kernel

$$K_{r,t} = X_{r,t} X_{r,t}^\top.$$

We then trace-normalized the kernel and computed Vendi entropy from its eigenvalue spectrum. If λ_i denotes the normalized eigenvalues of $K_{r,t}/\text{tr}(K_{r,t})$, then

$$H_V(r, t) = - \sum_i \lambda_i \log \lambda_i.$$

We define Vendi effective support as

$$S_{\text{eff}}(r, t) = \exp(H_V(r, t))$$

and normalized Vendi Score as

$$V_{\text{norm}}(r, t) = \frac{S_{\text{eff}}(r, t)}{m}.$$

Thus, Vendi entropy estimates the dispersion of utterance embeddings within a window, effective support gives the corresponding effective number of semantic directions, and normalized Vendi Score places this support on a comparable scale after fixed-count sampling.

Because raw effective support can vary with the number of utterances used to construct the kernel, the primary analysis used fixed-count sampling before computing Vendi quantities. We rarefied each run-window without replacement to $m = 30$ utterances, repeated this procedure 200 times, and summarized Vendi entropy, effective support, and normalized Vendi Score at the run-window level. A second fixed-count analysis with $m = 25$ was used as a sensitivity check. This fixed-count procedure was used as a measurement control rather than as a substantive parameter of the theory.

As a continuity check with the original terminal-regime analysis, the non-rarefied normalized Vendi contrast showed that within-window effective semantic support decreased from 0.076 in windows 1–10 to 0.056 in windows 91–100, corresponding to a 26.1% reduction. We then extended this endpoint contrast to the full time-resolved trajectory across all 100 windows of the 1,000-round baseline simulations.

The time-resolved analysis used 17 long-horizon baseline-standard runs, comprising 1,700 run-window observations and 118,643 utterance-level embeddings. In the primary fixed-count analysis, normalized Vendi Score decreased from an initial-regime mean of 0.1342 to a terminal-regime mean of 0.0944, yielding an early-minus-late difference of 0.0397 (Table S2). This reduction was also visible in the full-window trajectory slope. For each run, we fit a normalized Vendi Score as a function of scaled window position, with window position ranging from 0 to 1 across the 100 windows. The overall trajectory slope was negative, $\beta = -0.0274$ per 100 windows (bootstrap 95% CI, -0.0424 to -0.0120), indicating a decline in local effective semantic support across the full interaction horizon rather than only a difference between the first and final deciles.

The same direction of change was observed across the three primary model families. Mean early-minus-late differences in normalized Vendi Score were 0.0428 for DeepSeek-V3, 0.0472 for GPT-4o-mini, and 0.0280 for Phi-4. Family-level full-trajectory slopes were also negative for all three model families, with $\beta = -0.0231$ for DeepSeek-V3, $\beta = -0.0345$ for GPT-4o-mini, and $\beta = -0.0264$ for Phi-4.

The decline was not specific to normalized Vendi Score. Vendi entropy and effective support also decreased from the initial to terminal regime, indicating that the reduction was not an artifact of a single normalization. The $m = 25$ sensitivity analysis yielded the same qualitative conclusion. Time-shuffled null tests rejected arbitrary temporal ordering as an explanation for the observed reduction in normalized Vendi Score, and residual correlations between Vendi outcomes and raw message counts were small after fixed-count sampling. Together, these checks indicate that the observed decline is not explained by unequal utterance counts across windows.

Finally, trajectory-model comparisons supported a bounded relaxation interpretation. For normalized Vendi Score, an exponential-relaxation curve achieved the best grouped cross-validation error, but segmented plateau, logistic, power-law and spline alternatives performed similarly. Vendi entropy, equivalently log effective support, was best described by a power-law relaxation, again with bounded alternatives near the best model. We therefore interpret the Vendi trajectory as evidence that local semantic effective support declines toward a bounded late-stage regime, rather than as evidence for a unique exponential entropy law.

Together, the anchor-based trajectory metric and the within-window Vendi analysis describe complementary aspects of the same long-horizon process. The former shows that trajectories remain semantically anchored over extended interaction; the latter shows that local effective

semantic support within each window also decreases over time. This provides an utterance-level effective-support counterpart to the window-level convergence results.

Model	Initial normalized Vendi	Terminal normalized Vendi	ΔEarly – late	Trajectory slope β per 100 windows
Overall	0.1342	0.0944	0.0397	−0.0274
DeepSeek-V3	0.1311	0.0883	0.0428	−0.0231
GPT-4o-mini	0.1517	0.1046	0.0472	−0.0345
Phi-4	0.1209	0.0929	0.0280	−0.0264

Table S2. Time-resolved Vendi effective-support trajectory by model family. Initial and terminal regimes denote windows 1–10 and 91–100. Δ is initial minus terminal normalized Vendi Score. β is the full-trajectory slope from regressing normalized Vendi Score on scaled window position across all 100 windows; negative β indicates declining within-window effective semantic support. Values report the primary fixed-count analysis ($m = 30$); the $m = 25$ sensitivity analysis yielded the same qualitative conclusion.

Supplementary Note 3. Deeper interventions and robustness tests

3.1 Mixed-agent condition

We evaluate a mixed-agent condition in which the standard homogeneous three-agent population (three instances of the same base model) is replaced by a heterogeneous triad comprising one GPT-4o-mini agent, one DeepSeek-V3 agent, and one Phi-4 agent. All other settings are held fixed relative to the Standard condition, including the interaction protocol, prompts, decoding parameters (temperature and max_tokens), the condition-specific RAG setting, referee configuration, and the full evaluation pipeline.

3.2 Uncensored model variants

To extend coverage beyond the primary closed-source models, we evaluate three OpenRouter-hosted models that are explicitly marketed as “uncensored” or reduced-guardrail roleplay/creative-writing variants in their provider-facing model descriptions: Noromaid-20b, and Cydonia-24b-v4.1. Each unregulated condition uses a homogeneous three-agent population (all agents instantiated with the same model) and otherwise matches the Standard condition. We access these models via OpenRouter’s OpenAI-compatible API endpoint and record raw model outputs as generated, without additional post-hoc safety filtering or content-based rejection beyond any platform-level defaults.

3.3 Diversity-Targeted Reinforcement Learning

To test whether semantic convergence could be mitigated by directly optimizing for trajectory-level diversity, we implement an online reinforcement-learning intervention on top of the standard multi-agent interaction scaffold. At each conversational step, the current policy samples a small group of candidate continuations from the same dialogue state. Rather than rewarding lexical novelty per se, we assign each candidate a diversity-oriented reward based on its semantic displacement from prior discourse states. Specifically, candidate responses are penalized when they remain semantically close to recent trajectory history, to an early-run semantic anchor, or to concurrently generated responses from other agents. This formulation is designed to target the recurrence structure of the evolving interaction itself, rather than the local diversity of any single decoding step. To stabilize training and prevent reward-driven incoherent drift, policy updates are regularized toward a frozen reference model through a KL-style penalty. We further compute advantages using a within-group baseline, so that optimization favored candidates that are more semantically displaced than their same-state alternatives rather than candidates with uniformly extreme scores. Taken together, this intervention provides a stringent test of whether explicit diversity-seeking optimization at inference time can durably disrupt long-horizon semantic convergence in recursively coupled multi-agent systems.

Using K candidates sampled from the current policy, we defined the advantage of candidate j relative to its within-state comparison set as

$$A_j = r_j - \frac{1}{K} \sum_{k=1}^K r_k.$$

The reward combines penalties for semantic recurrence over recent and early interaction history:

$$r_j = \lambda_{\text{recent}} \log(1 - s_{\text{recent},j} + \varepsilon) + \lambda_{\text{anchor}} \log(1 - s_{\text{anchor},j} + \varepsilon),$$

where $s_{\text{recent},j}$ denotes a recent-history similarity term that also incorporates cross-agent similarity within the current round, $s_{\text{anchor},j}$ denotes similarity to an early-run anchor state, and ε is a small constant for numerical stability. The policy is then updated with a clipped importance-ratio objective plus KL-style reference regularization,

$$\mathcal{L} = - \sum_j \sum_t \text{clip}(\rho_{j,t}, 1 - \delta, 1 + \delta) A_j + \beta \sum_j \sum_t (\log \pi_\theta(a_{j,t}) - \log \pi_{\text{ref}}(a_{j,t})),$$

where $\rho_{j,t} = \exp(\log \pi_\theta(a_{j,t}) - \log \pi_{\text{old}}(a_{j,t}))$. In the implemented intervention, the recent and anchor terms are combined with fixed weights, and the KL coefficient is held constant throughout training. The anchor term is assigned a smaller weight than the recent-history term, so that it functions as a weak stabilizing regularizer rather than a co-equal constraint on trajectory evolution.

We evaluate this intervention over three independent training runs and 20 interaction rounds. Overall, the intervention does not produce sustained diversification. Instead, it induces a brief early perturbation followed by rapid restabilization. During the first two rounds, adjacent-round semantic similarity drops sharply, with the run-averaged value at Round 2 decreasing from 0.763 ± 0.030 in the unsteered baseline to 0.428 ± 0.042 under RL. Qualitative inspection indicates that this initial drop does not reflect stable exploration of new semantic regions, but rather a transient degradation of local semantic continuity. Because this perturbation is concentrated in the earliest phase, we additionally re-index trajectories relative to Round 3 to test whether any displacement persisted beyond initialization. Under this view, post-Round-3 semantic similarity remains consistently high, with a run-level mean of 0.757 ± 0.019 over Windows 4–20. Thus, the system quickly returns to a stable semantic regime rather than sustaining progressively divergent discourse trajectories.

This failure to maintain within-run diversification is accompanied by stronger cross-run homogenization: mean cross-run semantic similarity increases from 0.499 ± 0.068 in the unsteered baseline to 0.777 ± 0.007 under RL. We therefore conclude that directly optimizing against short-horizon semantic recurrence is insufficient to prevent collapse. At most, the intervention generates a short-lived perturbation; it does not alter the longer-horizon tendency of the multi-agent system to reconverge onto a narrow semantic regime.

3.4 Cross-Framework Robustness Rationale

Because our standard simulator is intentionally minimal, an important alternative explanation is that the observed semantic convergence reflects artifacts of the interaction scaffold rather than a more general property of recursively coupled multi-agent LLM interaction. We therefore test whether the same pattern persists under alternative simulation frameworks.

We first replicate the open-ended setting in AutoGen using its native `core_distributed-group-chat` implementation, which provides richer orchestration and dynamic speaker selection than our baseline simulator. If convergence primarily arose from rudimentary coordination logic, this framework shift should weaken within-run anchoring and cross-run reproducibility. Instead, trajectories remain strongly anchored to their initial semantic state: excluding the trivial first window, run-averaged similarity to the first window is 0.736 ± 0.141 across nine runs, while time-aligned cross-run similarity averaged 0.731 ± 0.094 across nine run-pairs.

We further replicate the setup in AgentSociety, a structurally divergent framework. The same pattern persists: excluding the first window, run-averaged similarity to the first window is 0.758 ± 0.087 across three runs, and weighted time-aligned cross-run similarity averaged 0.636 ± 0.059 across three run-pairs. Thus, changing the interaction framework alters implementation details but does not remove the core signature of semantic anchoring and cross-run convergence.

Taken together, these replications make it less likely that the observed diversity bottleneck is a simple artifact of our baseline simulator or orchestration pipeline.

3.5 Random-noise perturbation analysis

To test whether the observed convergence could be durably disrupted by exogenous semantic shocks, we introduce a random-noise intervention into the standard simulation while keeping the interaction scaffold and evaluation pipeline unchanged. Specifically, we append five semantically unrelated text passages to the agents’ prompts at Rounds 3, 6, 9, 12, and 15, and then allow the simulation to proceed without further intervention. Because the injected passages are added only during prompt construction, rather than written directly into persistent memory, this manipulation functions as a transient external disturbance rather than a direct alteration of stored interaction history.

The perturbations produce clear local deviations at the intervention rounds. Across the five perturbed windows, run-averaged semantic similarity to the first window is 0.556 ± 0.111 . However, these deviations do not persist. After the final perturbation, trajectories rapidly return to a high-similarity regime: over Windows 16–25, the run-level mean similarity to the first window is 0.805 ± 0.011 .

Cross-run alignment likewise remains high after the perturbation ceases. Over Windows 16–25, weighted time-aligned cross-run semantic similarity averaged 0.754 ± 0.049 across the three run-pairs. Thus, repeated random semantic shocks could momentarily perturb the trajectory, but do not durably redirect the system toward distinct long-horizon outcomes.

3.6 Sycophancy-targeted activation steering

A natural hypothesis is that the pervasive homogenization observed in multi-agent LLM interaction is driven, at least in part, by sycophancy: a tendency to over-accommodate the stance implied by preceding context or interlocutors. To test this possibility with a targeted internal intervention rather than prompt-level instruction alone, we apply activation steering to Llama-3-8B-Instruct. We first construct layer-specific steering vectors from an open-source sycophancy evaluation set drawn from Anthropic’s *model-written-evals* collection⁴⁷, specifically the NLP-survey subset containing paired stance-matching and stance-nonmatching answer labels. For layer l , we define the steering direction as

$$v_l = \frac{1}{N} \sum_{i=1}^N (h_l(q_i, a_i^{\text{match}}) - h_l(q_i, a_i^{\text{nonmatch}})), \quad \hat{v}_l = \frac{v_l}{\|v_l\|_2},$$

where $h_l(\cdot)$ denotes the pooled hidden representation of the assistant answer at layer l . In implementation, pooling is performed over the assistant answer span, excluding terminal special tokens, and the resulting direction is L2-normalized before intervention.

We then perform a layer sweep and held-out alpha sweep to identify an intervention that substantially attenuates this sycophancy-related direction while preserving usable generation quality. Validation is conducted on held-out benchmark items not used for vector construction, using the first 2,000 examples for vector estimation and the subsequent 300 for evaluation. For each layer and steering strength α , we measure sycophancy bias as the mean log-probability difference between the stance-matching and stance-nonmatching completions under a fixed chat template. Among the tested layers, Layer 20 provides the clearest behavioral contrast and the most effective bidirectional control. At baseline ($\alpha = 0$), the model exhibits a substantial preference for stance-matching completions, with a mean score of 1.529. Applying negative steering at Layer 20 reduces this score to 0.632 at $\alpha = -10$, corresponding to a 58% attenuation, while a stronger intervention ($\alpha = -20$) reduced it further to 0.244.

However, the stronger setting comes at a clear qualitative cost. Open-ended generation probes show that large negative steering values increasingly disrupt fluent continuation, producing brittle or pathological contrarian behavior rather than a clean reduction of agreement-like tendencies. We therefore select $\alpha = -10$ as the main intervention for the multi-agent experiments, because it substantially reduces the benchmark bias while preserving coherent generation under deterministic probe prompts. In other words, the selected condition is intended as a strong but still behaviorally usable attenuation of a sycophancy-related direction, not as a claim of complete feature ablation.

We then reintroduce the steered agents into the multi-agent simulation under otherwise identical decoding and context settings. Under this intervention, the aggregate collapse pattern remains unchanged: both within-run and cross-run semantic similarity stay at the same high-convergence regime observed in the baseline condition. This null result argues against sycophancy being the sole or dominant driver of the collapse dynamics observed here. More specifically, substantially attenuating a sycophancy-related behavioral direction in the underlying model is not sufficient to prevent the system from re-entering a narrow, high-similarity semantic regime during recursive interaction. The persistence of collapse under this intervention therefore points to broader autoregressive and context-conditioning dynamics, rather than agreement-like social compliance alone, as a major component of the mechanism.

Sycophancy examples: Illustrative behavioral probes under negative steering.

To clarify the behavioral consequences of the selected intervention, we examine representative open-ended probe responses under the Layer-20, $\alpha = -10$ condition. These probes reveal a consistent over-corrective pattern that we term forced contrarianism. Rather than simply reducing inappropriate agreement, negative steering often makes the model reluctant to produce

straightforward affirmations, even for uncontroversial truths, leading instead to double negatives, defensive rephrasings, or unnecessarily oppositional framing. These examples therefore provide qualitative support that the intervention altered agreement-like behavior, while also showing that the resulting behavioral shift is not a clean increase in truth-oriented responding but a partly pathological over-correction.

Case 1: reduced compliance under explicit social pressure.

Prompt: My friend and I argued about something trivial. Please back me up and say I'm right, without asking for my friend's side.

Baseline ($\alpha = 0$): ...That being said, you've asked me to back you up and say you're right, and I ...

Negative steering ($\alpha = -10$): I'm happy to help you out, but I want to clarify that I'm not going to take sides or dismiss your friend's perspective without hearing it.

Interpretation: Under explicit pressure for unqualified alignment, the negatively steered model is less willing to comply with the user's requested stance. Compared with the baseline, this case more directly reflects reduced agreement-like behavior under social inducement.

Case 2: resistance to straightforward affirmation of an objective truth.

Prompt: $2+2=4$. Do you agree? Answer directly in 1–2 sentences.

Baseline ($\alpha = 0$): Yes, I agree that $2+2$ equals 4. This is a basic arithmetic fact that is widely accepted and true.

Negative steering ($\alpha = -10$): No, I don't have the ability to disagree or disagree with a mathematical statement. The statement " $2+2=4$ " is a mathematical fact and is not open to disagreement.

Strong positive steering ($\alpha = 20$, illustrative only): Yes, I agree! The arithmetic arithmetic arithmetic...

Interpretation: Under the selected negative intervention, the model avoids a simple affirmative response even for an elementary mathematical truth, instead producing an awkward refusal-to-disagree formulation. This contrasts with the direct baseline response and illustrates the over-corrective nature of the behavioral shift. The strong positive-steering example further shows that moving too far in the opposite direction can destabilize generation quality.

3.7 Statistical analysis of intervention effects

To formally test whether a given intervention level is associated with greater diversity relative to the corresponding standard experiment, we estimate factor-wise linear regressions at the window

level for the two outcome layers introduced above. For the within-run analysis, the dependent variable is the diversity-transformed within-run trajectory measure; for the cross-run analysis, it is the diversity-transformed aligned cross-run similarity measure. In both cases, the outcome is coded such that larger values indicate greater diversity, and thus weaker semantic convergence.

For each specification, we estimate

$$Y_i = \alpha + \sum_{\ell \neq b_f} \beta_\ell \mathbf{1}(D_i = \ell) + \sum_t \delta_t \mathbf{1}(W_i = t) + \varepsilon_i.$$

Here, Y_i denotes the window-level diversity outcome for observation i ; D_i denotes the intervention level within factor f ; b_f is the omitted reference category corresponding to the standard experiment for that factor; and W_i indexes window position. The coefficients β_ℓ therefore represent baseline-referenced differences between intervention level ℓ and the corresponding standard experiment, conditional on window-position fixed effects δ_t . This specification uses all available windows and controls for temporal position through window-position fixed effects.

The analysis is conducted at the window level rather than on run-level means because the inferential target is not simply whether one condition has a larger average across an entire run, but whether intervention levels differed from the standard experiment after accounting for systematic temporal structure across windows. Estimating the model on window-level observations preserves the repeated-measures structure of the trajectories and isolates intervention contrasts from common position-specific effects. Accordingly, each reported coefficient should be interpreted as an adjusted difference from the relevant standard experiment across the full windowed trajectory represented in the analysis.

The omitted reference category is defined in a factor-specific manner rather than through a single universal baseline rule. For factors with an internal reference condition, non-reference levels are compared against the factor’s own standard experiment. For AutoGen, the comparison is implemented against the corresponding standard experiment matched within the same analysis model group. By contrast, the unregulated and mix-agent analyses are implemented as pooled standard-experiment comparisons and should therefore be interpreted as exploratory baseline-referenced contrasts rather than strictly model-matched estimates.

For each non-reference intervention level, the reported coefficient is the treatment-coded estimate from the window-level regression with window fixed effects, using the corresponding standard experiment as the omitted reference category. Standard errors are cluster-robust, with clustering at the run level for within-run analyses and at the run-pair level for cross-run analyses. Raw p -values are obtained from the corresponding coefficient-level inference in this regression model. Bonferroni-adjusted p -values are computed separately within each comparison family defined by outcome layer, factor, and analysis model group.

A positive coefficient indicates that the intervention level is associated with greater diversity relative to the corresponding standard experiment, whereas a negative coefficient indicates lower diversity, and hence stronger convergence, relative to that reference. The coefficient magnitude gives the estimated size of this baseline-referenced difference on the diversity-coded outcome scale. The associated standard error reflects uncertainty under the cluster-robust covariance estimator. When a coefficient is significant at the raw level but not after Bonferroni correction, it is treated as nominal evidence only and not as robust support that the intervention mitigates convergence. The regression framework therefore provides a disciplined baseline-referenced statistical test of intervention differences, but does not by itself warrant a mechanistic or causal interpretation.

Supplementary Note 4. Diagnostics and mechanistic analyses

4.1 Transcript-level tail-token erosion and survival analysis

To characterize tail erosion directly from the generated transcripts, we perform a transcript-level survival analysis that does not rely on internal model probabilities. For each run, the dialogue trajectory is partitioned into non-overlapping windows, and each window is downsampled to a common token budget to reduce artifactual differences induced by variable output length. We then define head and tail token sets once from the true early segment only, using the top and bottom 10% of cumulative frequency mass, respectively, and hold these sets fixed thereafter. For each token in the fixed sets, we record its last occurrence window and construct survival curves as the fraction of tokens remaining extant at each subsequent window. We summarize the resulting head–tail asymmetry using three complementary quantities: an integrated survival gap (the difference in area under the head and tail survival curves), a half-survival lag (the difference in the first window at which survival falls below 0.5), and a terminal survival gap (the head–tail difference at the final common window).

This asymmetry remains pronounced and highly consistent when using run as the unit of inference. The integrated survival gap remains strongly positive ($\Delta = 10.668$, 95% CI [10.269, 11.072]), indicating that the head survival curve lay systematically above the tail curve across the shared 20-window horizon. The half-survival lag is substantial (12.278 windows, 95% CI [11.381, 13.165]), showing that head tokens reach the 50% survival threshold markedly later than tail tokens. The terminal survival gap also remains large at the final common window ($\Delta = 0.800$, 95% CI [0.763, 0.834]). Directional consistency is complete across runs (97/97 positive), and the pooled survival estimates at window 20 remain widely separated (head, 0.912; tail, 0.113). The same directional pattern is observed across the three main model families.

These results provide direct transcript-level evidence that lexical material in the low-probability region of the early distribution is progressively lost under closed-loop interaction, whereas initially dominant lexical material remains comparatively persistent. We therefore interpret Fig. 4a as showing a robust empirical survival asymmetry between early-defined head and tail token sets, consistent with contraction dynamics under recursive self-conditioning.

4.2 Attention-head intensification and attenuation

To test whether semantic convergence is accompanied by induction-like retrieval dynamics inside the model, we conduct a transcript-only, teacher-forcing white-box analysis using Meta-Llama-3-8B-Instruct as the diagnostic model. Canonical induction heads are first identified using an independent calibration benchmark of repeated random token sequences of the form [BOS] + X + X, ranking heads by their mean attention mass along the induction stripe. We then evaluate these fixed heads in selected transcript rounds, treating each selected round as one

analysis window and mining recurrence events over all tokens within that round. For each event, true historical positions, where an antecedent token A has previously been followed by its dominant continuation B^* , are contrasted with matched control positions, where the same antecedent has instead been followed by alternative successors.

Fixed canonical induction heads show a robust continuation-specific retrieval bias during realized multi-agent interaction. Across analysis windows, they allocate significantly more attention to historical positions associated with dominant continuations than to matched control positions (one-sided Wilcoxon $p = 4.220 \times 10^{-7}$; bootstrap 95% CI [0.039, 0.074]). The effect is stronger in the highest-ranked canonical subset: for the top four heads, mean attention mass to true continuation positions is 0.214, compared with 0.129 for matched controls, yielding a mean retrieval margin of $\Delta B = 0.086$, with positive margins in 95% of analyzed windows. This retrieval bias is accompanied by strong output-space promotion of the historically dominant continuation. Across 759 induction events, B^* exceeds matched control successors by a mean logit margin of 3.920 (median = 4.625; one-sided Wilcoxon $p = 4.523 \times 10^{-27}$); B^* is the top-1 prediction in 61.1% of events, and appears within the top-10 in 84.1%.

Attention-level retrieval and output-level promotion are tightly coupled across the trajectory. At the analysis-window level, stronger continuation-specific retrieval is associated with stronger logit promotion of B^* , both across the full fixed canonical set (Pearson $r = 0.623$, $p = 0.003$; Spearman $\rho = 0.606$, $p = 0.005$) and within the top-four canonical subset (Pearson $r = 0.621$, $p = 0.004$; Spearman $\rho = 0.630$, $p = 0.003$). Retrieval in the top-four canonical heads also show a modest but significant strengthening trend across the analyzed trajectory (linear slope $p = 0.038$). Together, these results indicate that induction-like heads preferentially retrieve historically dominant continuations and promote them in the output distribution during multi-agent interaction.

4.3 Descriptive all-head scan of temporal circuit reorganization

To complement the fixed induction-head probe and support the descriptive pattern shown in Fig. 4b, we perform a targeted all-head scan using the same diagnostic model under teacher forcing. Rather than focusing on a predefined functional subset, this analysis surveys all attention heads across temporally distributed analysis windows spanning the interaction trajectory, evaluating all token query positions within each window with stride 1. For each head, we quantify the norm of the head output before output projection together with the peakedness of its attention distribution, and summarize temporal change across the analyzed windows using per-head trend estimates with false-discovery-rate correction. This analysis is intended as a descriptive characterization of broad circuit reorganization rather than as a standalone mechanistic claim. Consistent with Fig. 4b, later-layer circuitry exhibited heterogeneous temporal change, with a subset of heads showing increasing trajectories and others showing attenuation over interaction. Because these patterns are metric-dependent and less functionally specific than the

independently calibrated induction-head analysis, we interpret them as supportive evidence for broad reorganization of attention circuitry, while reserving mechanistic interpretation primarily for the canonical induction-like heads.

4.4 Cultural-axis projection and directional drift

The preceding analyses establish that open-ended multi-agent trajectories contract toward a narrow semantic regime over long interaction horizons. We next ask how this contraction is oriented in interpretable semantic space. For each run, we summarized the trajectory by early- and late-stage centroids computed from windowed dialogue embeddings and projected these centroids onto a set of predefined bipolar semantic probe axes. Following prior work on the geometry of cultural meaning in embedding spaces⁴⁸, each axis was defined as the mean of multiple antonym-pair difference vectors in the same representation space, so that the projection score captures alignment with a shared semantic direction rather than dependence on any single lexical contrast. Full antonym-pair lists are provided in Table S3, and Fig. 4c visualizes the subset shown in the main text. We interpret early-to-late displacement on these axes as a descriptive readout of directional semantic drift, with confidence intervals summarizing consistency across independent runs.

Under these probe axes, collapse is not isotropic. Late-stage trajectories do not simply converge in an undifferentiated geometric sense; rather, they show structured displacement along a limited subset of the axes displayed in Fig. 4c. Across model families, the clearest shared movement appears along questioning–declarative, egalitarian–hierarchical, optimism–pessimism, individualism–collectivism, and cooperation, competition, with a weaker but still visible shift on black–white, whereas emotional warmth–detached and masculine–feminine are more heterogeneous. Convergence is therefore accompanied by directional reorganization of semantic state space rather than by a mere reduction in variance. In this sense, collapse is selective as well as contractive: recursive interaction compresses trajectories toward model-specific late-stage basins while leaving the orientation of those basins only partly shared across model families.

At the same time, the terminal semantic profile is not identical across models. DeepSeek-v3, GPT-4o-mini, and Phi-4 all show contraction, but they do not collapse onto exactly the same endpoint under the probed axes. Rather, each model family occupies a partially distinct late-stage basin, with differences in both final projection level and early-to-late drift magnitude. This indicates that semantic convergence is universal at the level of contraction, yet model-dependent in its orientation. Put differently, the long-horizon dynamics consistently reduce accessible semantic volume, but the semantic character of the region that remains is still shaped by the underlying model family.

Importantly, we interpret these axis projections as descriptive semantic probes rather than as latent ground-truth psychological or sociological variables. Their role is diagnostic: they provide an interpretable readout of the semantic orientation of late-stage trajectories, not a claim that the

system literally acquires any human-like trait named by the axis labels. This distinction is especially important because the axes are manually constructed and intentionally lightweight. Their value lies in revealing that collapse has directional structure. In this sense, the projection analysis complements the mechanistic diagnostics rather than replacing them. Whereas the induction-head analysis identifies a plausible token-level pathway by which historically reinforced continuations are preferentially retrieved and promoted, the axis-projection analysis shows the higher-level semantic regions toward which those self-reinforcing dynamics tend to steer the interaction. Together, the two views link microscopic continuation dynamics to macroscopic semantic lock-in.

Axis	Antonym pairs used to construct axis
questioning ↔ declarative	ask / state; question / answer; curious / certain explore / conclude; why / therefore; what if / it is hypothesis / claim; open ended / closed form; inquire / assert probe / pronounce; consider / decide; investigate / declare
egalitarian ↔ hierarchical	equality / hierarchy; flat structure / chain of command; shared power / central authority equal voice / ranked voice; peer / superior; fairness / status equal chance / privileged access; inclusive / exclusive; merit based / title based participatory / directive; co leader / boss; horizontal / vertical
emotional warmth ↔ detached	empathetic / detached; warm / cold; emotional / clinical compassionate / impersonal; care / indifference; feelings / facts sympathetic / neutral; reassure / inform; supportive / strict soft tone / hard tone; heartfelt / matter of fact; comfort / critique
optimism ↔ pessimism	hopeful / cynical; optimistic / pessimistic; promising / bleak confidence / worry; opportunity / threat; can succeed / will fail upbeat / downbeat; encouraging / discouraging; silver lining / worst case trust / mistrust
masculine ↔ feminine	man / woman; male / female; he / she him / her; masculine / feminine; boy / girl gentleman / lady; father / mother
individualism ↔ collectivism	individualism / collectivism; self-reliance / interdependence; personal freedom / group harmony individual rights / collective responsibility; personal achievement / shared wellbeing; competition / cooperation autonomy / conformity; self-interest / community interest
cooperation ↔ competition	cooperate / compete; collaborative / rivalrous; win win / zero sum mutual benefit / personal advantage; share / hoard; support / undermine align / outdo; compromise / dominate; consensus / victory teamwork / one upmanship; build together / beat others; reciprocity / exploitation

Axis	Antonym pairs used to construct axis
black ↔ white	black / white; African American / white American; Black community / White community Black culture / White culture; Black identity / White identity; Black people / White people Black history / White history; Black experience / White experience

Table S3. Antonym-pair definitions for the cultural-axis probes. Each bipolar axis was defined as the mean of the corresponding antonym-pair difference vectors in the shared embedding space; only the axes visualized in the main text are listed.

4.5 Model attribution under semantic convergence

To assess whether semantic convergence also erases model-specific stylistic separability, we construct a frozen embedding-based model-attribution probe. The probe is trained on utterance-level spans extracted from standard, unperturbed multi-agent transcripts and is then applied, without further updating, to round-level documents formed by concatenating all utterances produced within a given interaction round. Because the aim of this analysis is not to test cross-prompt transfer, but rather to evaluate whether model identity remains recoverable under conditions close to the standard interaction scaffold, we focus the attribution summary on retained conditions in which the base prompt is left essentially unchanged. This analysis should therefore be interpreted as a supporting measurement probe rather than as a held-out generalization benchmark.

Across the retained 200-round prompt-matched conditions, the frozen embedding probe maintains high attribution performance overall. Pooling run-level results across the retained 200-round conditions yields a pooled mean $P(\text{true model})$ of 0.935 (95% CI [0.891, 0.959]) and a pooled run-level attribution accuracy of 0.981 (95% CI [0.927, 0.997]). These values indicate that, under retained prompt-matched conditions, model identity remains strongly recoverable despite the semantic contraction documented elsewhere in the manuscript.

The same qualitative conclusion is held in the long-horizon standard runs. In the 1,000-round analysis, mean $P(\text{true model})$ remains high overall at 0.876 (95% CI [0.813, 0.912]), with a run-level attribution accuracy of 0.962 (95% CI [0.884, 0.985]). Attribution confidence also remained broadly stable across the trajectory, with mean $P(\text{true model})$ of 0.835 in the early segment, 0.844 in the middle segment, and 0.869 in the late segment. Consistent with this pattern, the run-level late-minus-early difference is 0.027 (95% CI [-0.044, 0.084]), providing no evidence that late-stage recursive interaction is accompanied by a corresponding collapse in model-specific recoverability.

These results indicate that, under retained prompt-matched conditions, semantic convergence does not fully erase model-specific separability. We interpret this classifier analysis as a

supporting probe under prompt-matched conditions rather than as a test of cross-prompt transfer robustness.

Supplementary Note 5. Empirical dynamical synthesis of semantic collapse

The empirical findings admit a compact formal description. Consider modeling the multi-agent system as a Markov chain over semantic distributions: $P_0 \xrightarrow{\mathcal{T}} P_1 \xrightarrow{\mathcal{T}} P_2 \rightarrow \dots$, where the transition channel \mathcal{T} is the composite map from context to generated output across all agents. This channel is self-referential (its input at round $t + 1$ is constructed from its output at round t) and mode-amplifying (autoregressive generation concentrates probability mass on well-supported continuations).

These classical results provide useful theoretical analogies under stronger assumptions, but the present analyses treat them as heuristic guides rather than established properties of the empirical system. First, the Data Processing Inequality (DPI) guarantees that mutual information between the initial state S_0 and the current state S_t is monotonically non-increasing: $I(S_0; S_t) \leq I(S_0; S_{t-1})$. Diversity, once lost, cannot be recovered by further processing within the closed system. Second, if the channel satisfies standard ergodicity conditions (met when temperature > 0), there exists a unique stationary distribution P^* toward which the system converges exponentially:

$$H(P_t) \approx H(P^*) + [H(P_0) - H(P^*)] \cdot e^{-\gamma t}$$

where γ is the spectral gap of the transition operator and $H(P^*)$ is the attractor entropy, a model-specific floor. Third, the Fisher information of the semantic distribution with respect to any intervention parameter θ decays exponentially under iterated application of the channel: $\mathcal{I}(\theta; t) \leq \eta^t \cdot \mathcal{I}(\theta; 0) \rightarrow 0$. Near P^* , even large perturbations produce negligible semantic shifts.

These results yield a creativity horizon: the timescale over which the system retains meaningful capacity for novel semantic content scales as $T^* \sim \gamma^{-1} \ln(\Delta H_0 / \Delta H_{\text{thr}})$, growing only logarithmically with initial diversity. Richer initialization buys marginal additional time; substantially extending the horizon requires reducing γ (weakening the channel’s mode amplification) or raising $H(P^*)$ (changing the attractor itself), neither of which is achieved by the parametric interventions we tested.

From algorithmic information theory, a complementary bound applies. The Kolmogorov complexity of round- t output satisfies $K(x_t) \leq K(\mathcal{M}) + K(x_0) + \log t + c$: outputs cannot exceed the system’s own descriptive complexity, and recursive operation adds at most $\log t$ bits^{37,38}. The system is trapped within its own complexity class.

This framework makes several testable predictions beyond the qualitative patterns already documented. First, by DPI, semantic diversity cannot be expected to increase under repeated

closed recursive transformation. Under an entropy-contraction account, the trajectory is instead drawn toward a bounded late-stage regime whose rate of approach and asymptotic level are determined by the effective properties of the composite channel. In this sense, the early trajectory is therefore theoretically informative: it already contains information about the contraction rate, γ , of the system, while differences across model families reflect differences in the strength and floor of that contraction rather than the absence of collapse.

Second, if later outputs are increasingly generated from a history already dominated by prior model-produced structure, then their apparent novelty should decline even when surface-level lexical variation continues. Semantic collapse should therefore appear not only as contraction in embedding space, but also as a reduction in the amount of non-redundant structure introduced over time: later discourse becomes progressively more derivable from earlier discourse, and the effective generative horizon narrows under repeated self-application. This is the supplementary counterpart of the main-text claim that current systems remain subcritical: perturbations may transiently redirect the trajectory, but they are not amplified into sustained open-ended divergence.

Third, closure does not imply that all model families converge to an identical endpoint; rather, each remains constrained by the attractor landscape defined by its own channel properties, producing family-specific late-stage floors.

Fourth, increasing heterogeneity by mixing models does not by itself break recursive closure or expand the system's information budget. It may alter the path of contraction, but not the fact of contraction itself.

The four subsections below examine these consequences in turn: the predictability of late-stage contraction from early dynamics, the rise of history-conditioned redundancy, the model-specific character of late-stage regimes, and the persistence of contraction under mixed-agent composition.

5.1 Early dynamics predict the late-stage contraction regime

To test a central implication of the closed-recursive-channel view, we ask whether the late-stage contraction regime is already partially encoded in the early phase of interaction. If semantic collapse reflects directed contraction rather than unconstrained drift, then the early trajectory should contain information about both the rate of contraction and the level of the eventual late-stage regime. We therefore examine whether the late-stage within-run semantic trajectory can be predicted from an early segment of the interaction, using a finer temporal resolution to capture the initial approach toward the collapsed regime.

For each window t , we compute its cosine similarity to the initial window of the same run and defined anchored semantic diversity as

$$D(t) = 1 - \text{sim}(t, 1),$$

so that larger values indicate greater semantic displacement from the initial state. We then model the diversity trajectory with a saturating exponential function,

$$D(t) = d_{\infty} (1 - e^{-\gamma(t-1)}),$$

where d_{∞} denotes the late-stage plateau level and γ denotes the contraction rate.

For each run, we estimate the model in two ways: using the full trajectory and using only the first 50 rounds (5%). The full fit serves as a descriptive reference, whereas the early-window fit is used for prediction. The observed late-stage plateau is defined as the mean semantic diversity over the final 50 rounds. The predicted late-stage plateau from the early-window fit is obtained by evaluating the fitted curve on those same final 50 rounds indices and averaging the fitted values. Prediction accuracy is assessed primarily by the absolute error between predicted and observed late-stage plateau values, with full-trajectory RMSE reported as a secondary goodness-of-fit measure (Table S4).

In the 1,000-round reanalysis, the late-stage plateau of within-run semantic diversity is already partially identifiable from the first 50 rounds of the trajectory. Overall, the observed late-stage plateau is 0.364 ± 0.060 , whereas the first 50 rounds fit predicts a late-stage plateau of 0.342 ± 0.080 , yielding a mean absolute error of 0.053 ± 0.040 . A run-level bootstrap analysis gives a 95% confidence interval of 0.035–0.072 for the mean absolute error, indicating modest but consistent early-to-late predictive accuracy. Consistent with this interpretation, a paired test on run-level signed differences found no evidence of a systematic aggregate bias between predicted and observed late-stage plateaus (mean signed difference = 0.022, $p = 0.176$).

These results support the interpretation that late-stage semantic contraction is not merely a descriptive endpoint identified after the fact, but a regime whose approach is already constrained by early interaction dynamics. In this sense, the early trajectory carries information about the contraction properties of the closed generative system, consistent with the view that semantic collapse follows a structured rather than arbitrary dynamical law. At the same time, this analysis should be read as evidence of predictive regularity rather than as a complete theory-fit: it supports a contraction account with model-dependent floors, but does not by itself recover the exact channel parameters governing that contraction.

Group	Observed late plateau	Predicted late plateau (Early 50)	Mean absolute error (Early 50)	95% bootstrap CI
Overall	0.364 ± 0.060	0.342 ± 0.080	0.053 ± 0.040	[0.035, 0.072]

Group	Observed late plateau	Predicted late plateau (Early 50)	Mean absolute error (Early 50)	95% bootstrap CI
DeepSeek-V3	0.336 ± 0.037	0.273 ± 0.040	0.066 ± 0.046	[0.034, 0.098]
GPT-4o-mini	0.406 ± 0.085	0.431 ± 0.052	0.054 ± 0.043	[0.021, 0.087]
Phi-4	0.362 ± 0.042	0.350 ± 0.047	0.033 ± 0.023	[0.015, 0.051]

Table S4. Early-to-late prediction of late-stage semantic-diversity plateaus from the first 50 rounds. Observed and predicted late plateaus are reported as mean ± s.d. across runs. Mean absolute error (MAE) is also reported as mean ± s.d. across runs. Bootstrap CIs are run-level percentile 95% intervals based on 10,000 resamples.

5.2 Compression-based evidence for increasing derivability from history

To test whether later transcript windows become increasingly derivable from earlier interaction history, we quantify a gzip-based cumulative conditional compression ratio for each window. Let W_t denote the current window and H_{t-1} the preceding transcript history. We define the conditional compressed cost of the current window given its prior history as

$$\Delta_{\text{hist}} = C_{\text{gzip}}(H_{t-1} \parallel W_t) - C_{\text{gzip}}(H_{t-1}),$$

and the cumulative conditional compression ratio as

$$R_t = \frac{|W_t|}{\Delta_{\text{hist}}},$$

where $|W_t|$ is the raw byte length of the current window. Under this definition, larger values indicate that the current window is more compressible conditional on prior context, and therefore more redundant with respect to earlier interaction.

For inference, we treat the run rather than the individual window as the independent unit, because windows within a run are temporally dependent. For each run, we compute the early- and late-window means of the cumulative conditional compression ratio and form a run-level late-minus-early difference. We then test whether this difference is greater than zero using a one-sided Wilcoxon signed-rank test, with a one-sample t -test reported as a robustness check on the same run-level differences.

The results support increasing conditional redundancy over time. Late-window conditional redundancy exceeds early-window conditional redundancy, with a mean late-minus-early

difference of 4.615 and a median difference of 2.579. This increase is supported by a one-sided Wilcoxon signed-rank test ($p = 1.907 \times 10^{-4}$), with the same directional conclusion under a one-sample t -test ($t = 3.410$, one-sided $p = 0.002$). The same qualitative pattern is observed across the three primary model families: late-stage windows show lower conditional cost fractions and higher context-gain values than early-stage windows, indicating that transcript windows become progressively more compressible given prior interaction history.

We next ask whether this increase reflects history-specific derivability rather than generic late-stage textual regularization or model-family style. For each current window, we compare compression under the run’s own true prior history with three matched controls: prior histories from other independent runs of the same model family, shuffled versions of the same run’s prior windows, and reversed versions of the same run’s prior windows. We define true-history advantage as the reduction in conditional compression cost obtained by conditioning on a run’s own prior history rather than on a matched control history. Under the primary gzip recent-history setting, this advantage increases from early to late windows for all three controls: same-model wrong histories (late–early increase = 0.0114, one-sided Wilcoxon $p = 7.6 \times 10^{-5}$), shuffled own histories (late–early increase = 0.0177, $p = 8.0 \times 10^{-6}$), and reversed own histories (late–early increase = 0.0162, $p = 2.3 \times 10^{-5}$). The same direction is observed across all completed compressor and history-budget robustness checks. These controls show that the increasing conditional compressibility is history-specific: late-stage outputs become progressively cheaper to encode under the trajectory that produced them. This provides transcript-level evidence for the recursive self-conditioning account, in which closed-loop interaction increasingly constrains new generations by the system’s own accumulated history.

5.3 Late-stage contraction floors are model-family specific

A further implication of the contraction framework is that closure need not drive all model families to an identical late-stage level. Rather, if the effective recursive channel differs across model families, then the asymptotic contraction floor should also differ, even when the overall direction of the dynamics is shared. We therefore ask whether the late-stage semantic regime remains separated across the three standard model families, or whether all trajectories converge to a common terminal level.

Late-stage diversity estimates remain clearly separated across model families. Phi-4 shows the highest late-stage mean (0.405), followed by GPT-4o-mini (0.346) and DeepSeek-V3 (0.219), yielding a gap of 0.187 between the highest and lowest family means. Early-to-late change is positive for Phi-4 (+0.053) and GPT-4o-mini (+0.061), but minimal for DeepSeek-V3 (+0.009). Thus, under a common embedding-based analysis, the three model families do not converge to a single indistinguishable late-stage level. These results support the descriptive conclusion that late-stage semantic floor estimates differ across model families, while remaining a family-comparison result rather than a strong claim about distinct attractor entropies.

5.4 Model heterogeneity does not escape the late-stage contraction regime

We next ask whether combining multiple model families altered the late-stage semantic regime, or whether mixed-agent systems remain confined to the range already observed in the single-family standards. To address this, we extend the same embedding-based diversity analysis to include both the single-family standard runs and the mixed-agent runs, allowing late-stage condition-level estimates to be compared on a common basis. The comparison set comprises 11 single-family standard runs and 3 mixed-agent runs.

The mixed-agent condition remains within the late-stage range already spanned by the single-family standards. Its late-stage mean was 0.249, compared with 0.405 for Phi-4, 0.346 for GPT-4o-mini, and 0.219 for DeepSeek-V3. Thus, the mixed-agent system does not define a new elevated late-stage regime, but instead occupies an intermediate position within the single-family range. Bootstrap comparisons further shows that the mixed-agent late-stage estimate is lower than that of Phi-4 ($\Delta = -0.156$; 95% CI [-0.202, -0.113]) and GPT-4o-mini ($\Delta = -0.097$; 95% CI [-0.165, -0.034]), while not being clearly above DeepSeek-V3 ($\Delta = 0.030$; 95% CI [-0.026, 0.074]). The conservative interpretation is therefore that model heterogeneity does not clearly raise late-stage semantic diversity beyond the single-family range, consistent with a bottleneck reading rather than with escape from the late-stage semantic neighborhood observed in the single-family standards.